RICE UNIVERSITY

SPACE SCIENCE 400 - LECTURE NOTES

19. Lectures on Cosmic Rays

19.1 Definitions and description of primary cosmic rays.

The term "cosmic-radiation" was first applied by Millikan and Regener, in the 1920's, to the penetrating ionizing radiation that apparently reached the earth from outside its atmosphere. Since then the meaning of the term has evolved as knowledge of the phenomena associated with extra-terrestrial radiation has increased. A good current definition is that cosmic-rays are those charged particles which reach the earth's magnetosphere from interplanetary space with velocities greater than the solar wind velocity of ~ 400 km/sec (corresponding to a proton energy of ~ 1 keV and an electron energy of ~ 0.5 ev). The term often includes the energetic neutral particles, neutrinos and neutrons, but does not usually mean the photons of radio, optical, x or gamma radiation, although these latter radiations are closely related to the origins of cosmic rays.

Cosmic radiation is conveniently classified according to its source. Galactic cosmic rays reach the earth from outside the solar system, where their flux is thought to be isotropic and constant over periods of at least tens of thousands of years. The particles have energies from about 10^7 ev (or perhaps lower) to at least 10^{19} ev. In approaching the earth's orbit the number with energy below ~ 15 Bev that reach the earth's orbit is reduced by the solar wind and interplanetary magnetic field so that the more active the sun, the fewer of these low energy

particles are observed at the earth. The flux of higher energy particles at the earth remains constant. The maximum flux of galactic cosmic rays observed at earth (which occurs when the sun is in the quiet part of its 11 year cycle) may equal the interstellar flux, but it could be that the number of lower energy particles is always depressed at the earth's orbit, since there is always some solar wind. Hence we will describe the galactic cosmic rays observed within the solar system and then consider the result of supposing that the interstellar flux equals the maximum flux observed.

Figure 1 shows the integral energy spectrum of particles observed at the earth.

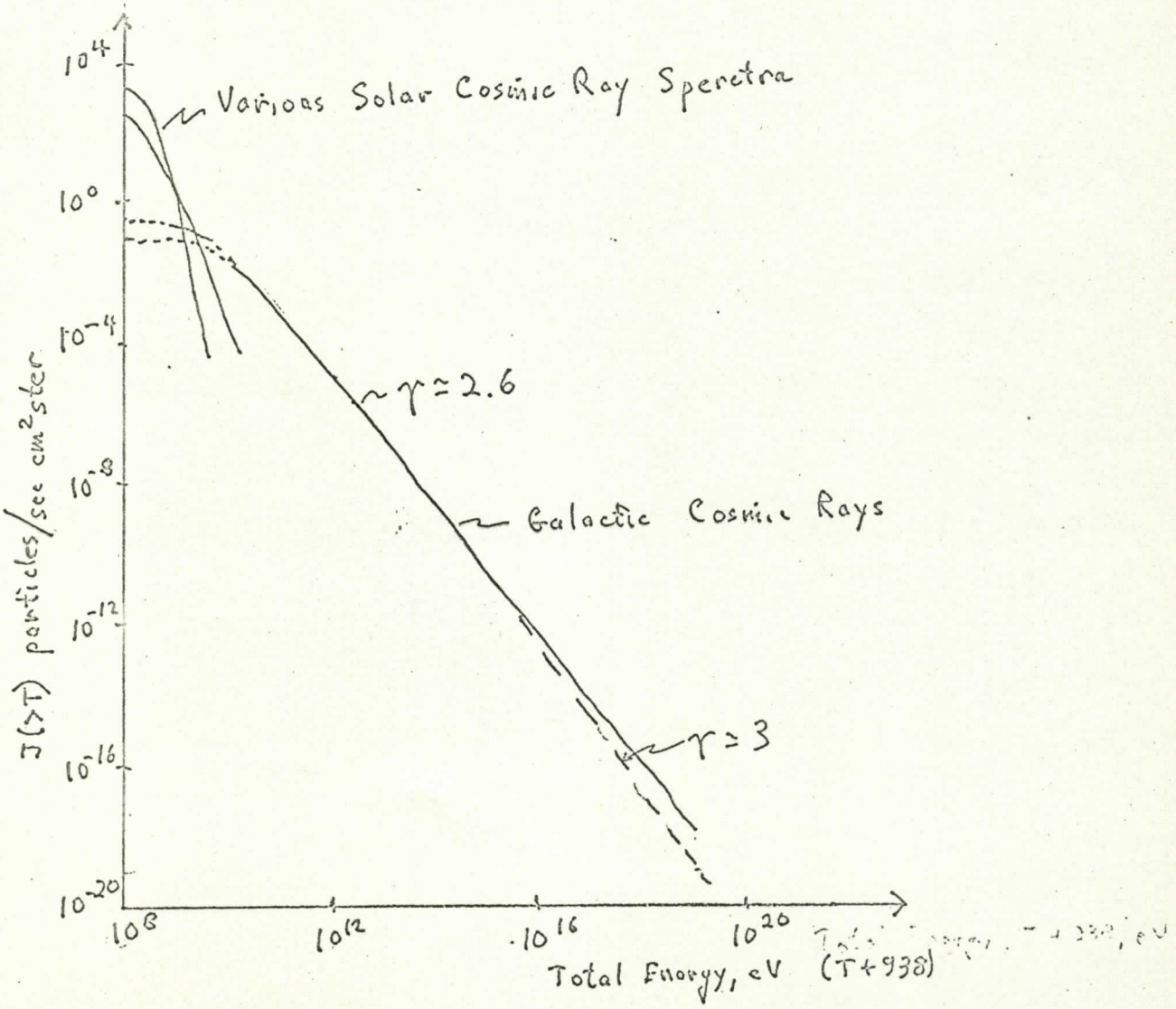

Figure 1.

Above 2×10^9 ev the spectrum is well represented by $J(>T) = K/(T + .938)^{\gamma-1}$ the values of γ appear in Figure 1. The differential energy spectrum is

$$-\frac{d}{dE} J(>T) = K(\gamma-1)/(T + .938)^{\gamma} \text{ particles/cm}^2 \text{ sec ster MeV}$$

where T = is the kinetic energy/nucleon in BeV, and the flux of all nuclei $J(>500 \text{ MeV}) \simeq 0.25/\text{cm}^2$ sec ster.

Although the majority of cosmic rays are protons, heavier nuclei are observed, and their energy spectrum has the same dependence upon T, i.e., the same index γ, over the range $\sim 2 \times 10^9$ to $\sim 10^{11}$ ev/nucleon. The charge spectrum (that is, the relative abundance of different nuclei) is not known at higher energies, and at the lower, non-relativistic energies the energy spectrum is different for different kinds of nuclei. We will discuss this point in detail later. Table I lists the fluxes of galactic cosmic rays with energies above 2,4 BeV/nucleon (Waddington, 1960). The abundances in the sun and in solar cosmic rays (mostly 50-200 MeV/nucleon), taken from Biswas and Fichtel (1965), are presented for comparison. The number of relativistic (T>1 MeV) electrons among galactic cosmic rays amounts to a few percent of the proton flux.

We will return to the problem of cosmic ray composition later, and now describe solar cosmic rays. Unlike the galactic particles, these are produced by the sun, and this happens only occasionally in those violent outbursts which also produce optical flares, radio noise, and x-rays. The particles reach the earth a few minutes to an hour after the solar eruption, the more energetic (faster) ones arriving first. Typically the peak intensity is

reached one or two hours after the first arrival, and then the flux disappears in a period of a few days, with the more energetic particles declining more rapidly than the softer (slower)ones. Therefore, the energy spectrum varies during an event, and is also quite different in different events. The integral energy spectrum may be written $J(>T) = K(T + .938)^{\gamma-1}$ with T>1 BeV and γ = 4 to 10, but at lower energies this fails and a form such as $J(>T) = AT^{-m}$, with m = 4 to 10 is required. The integral energy spectrum rises with decreasing energy down to T = 10 MeV, and possibly lower. In very large events, relativistic particles appear but frequently only slower particles are detected. The ratio of protons to heavier nuclei varies from one event to another, but the relative abundance of nuclei with Z>2 is usually about that shown in Table I. The electron flux is at most a few percent of the proton flux. The peak intensity of all particles with T>10 MeV ranges from 1 to $10^4/cm^2$ sec ster.

Although the major research problems in cosmic ray physics today are the measurement of these primary fluxes and the explanation of them in terms of astrophysical processes, we will first consider the relationship between cosmic rays and the other phenomena and will return to astrophysical considerations at the end.

19.2 Relationship to Other Areas of Research

The study of cosmic rays has been and/or is related to research in several other areas which are outlined below.

A. The interaction of high energy particles and the nature of unstable, elementary particles:

1. Positrons, π and μ mesons, and some heavier particles were discovered among cosmic ray secondaries in the atmosphere.

2. Some of the processes explained by quantum electrodynamics such as pair production, and positron annihilation were first observed in the electron-photon cascade.

3. Currently cosmic rays are the only source of particles with energies above ~ 30 BeV.

B. Various effects of the action of cosmic rays on matter and on the geomagnetic field

1. Radioactive nuclei and spallation products are produced in meteors when cosmic rays bombard them in space. From the distribution of these elements in fallen meteorites it is possible to estimate

a) The size of the meteor before it passed through the atmosphere

b) The age of the meteor

2. Cosmic ray secondary neutrons produce C^{14} in the atmosphere. By measuring the distribution and concentration of this isotope it is possible to

a) Calculate the length of time organic material has been dead.

b) Estimate the rate at which the atmosphere circulates and mixes with the biosphere and oceans.

3. The distribution of cosmic rays over the earth results from the configuration of the geomagnetic field. Changes in the latter can be deduced from changes in the former.

4. Upward moving cosmic-ray secondaries which decay in flight are one source of trapped radiation.

C. Processes in the outer portion of the sun and in interplanetary space.

1. The composition of solar cosmic rays is related to the composition of the sun, where the particles are accelerated.

2. The energy spectra and temporal variations of solar cosmic rays are intimately related to the processes in sunspots and other active regions of the sun. Models of solar activity must account for cosmic rays as well as the radio, optical, and x-ray bursts from the sun.

3. The interplanetary magnetic field determines the time variations of solar cosmic rays at the earth is part and, it is thought, causes all the temporal variations observed in galactic cosmic rays.

D. Extra-solar astrophysical processes.

1. The energy density of galactic cosmic rays is ~ 1 ev/cm^3 and is about equal to that of starlight and of the estimated interstellar magnetic field. Thus, depending upon cosmic ray lifetime, a significant amount of stellar energy may go into accelerating cosmic rays.

2. Galactic cosmic rays provide the only direct sample of extra-solar system nuclear abundance. The abundance is determined by the source of the rays and by the amount of matter with which they have collided since acceleration.

3. The energy spectrum and isotropy is related to the interstellar magnetic field strength.

4. The galactic electron spectrum must agree with the measured synchrotron radio noise from the galaxy.

TABLE I. Abundance of Elements

Relative to $O^{16} = 1.0$

Biswas & Fichtel, Space Sci Rev 4, 709-736 (1965)

Element	Z	Solar Cosmic Rays	Sun	Universal Abundance	Galactic Cosmic Rays
H	1	Variable		1950	810
H_e	2	107 ± 14		150	48
Li	3	----	$<10^{-5}$	$<10^{-5}$	0.3
Be,B	4,5	<.02	$<10^{-5}$	$<10^{-5}$	0.8
C	6	.59 ± .07	0.6	0.26	1.8
N	7	.19 ± .04	0.1	0.20	$\lesssim$0.8
O	8	1.0 (Defn)	1.0	1.0	1.0
F	9	<.03	.001	$<10^{-4}$	$\lesssim$0.1
Ne	10	.13 ± .02		0.36	0.3
Na	11		.002	0.002	0.19
Mg	12	.043 ± .011	.027	.040	0.32
Al	13	----	.002	.004	.06
Si	14	.033 ± .011	.035	.045	.12
15 - 21		.057 ± .017	.032	.024	.13
22 - 28		$\lesssim$ .02	.006	.033	.28

Galactic Cosmic Rays

Waddington, Prog Nucl. Phys 8, 1-45 (1965)

Flux (Above 2.4 Bev/nucleon) particles/m^2 sec ster	Element Group
1510 ± 150	P
89 ± 3	α
2.0 ± .2	L
5.6 ± 0.2	M
1.88 ± .3	H($10 \leq z \leq 19$)
.69 ± .16	VH($20 \leq z \leq 28$)
200	Electrons 3-8 MeV

RICE UNIVERSITY

SPACE SCIENCE 400 - LECTURE NOTES

19.3 Review of Particle Physics - Cosmic Rays

In order to understand cosmic radiation it is necessary to understand how the particles comprising primary and secondary cosmic rays interact with matter; i.e., with protons, neutrons, and electrons. The more important (for our purpose) particles are listed in the attached table. Electrical charge, denoted by superscript in the first column, is $\pm$ one electronic charge $= \pm 1.6 \times 10^{-19}$ coulombs. Mass is expressed in units of the electron mass, or more conveniently by the rest mass energy, $E_o = Mc^2$, where M = rest mass.

Motion is characterized by direction, of course, and by the speed relative to the velocity of light, $\beta = v/c$, where $c \simeq 3.00 \times 10^{10}$ cm/sec. Related to β are

$$\text{momentum, } pc = \frac{Mc^2\beta}{\sqrt{1-\beta^2}} ,$$

$$\text{kinetic energy, } T = \frac{Mc^2}{\sqrt{1-\beta^2}} - Mc^2 ,$$

where M is the rest mass. The total energy, E is related to these by

$$E = \sqrt{(pc)^2 + (Mc^2)^2} = \frac{(Mc^2)}{\sqrt{1-\beta^2}} = T + Mc^2$$

The momentum is a three-dimensional vector of magnitude pc, and $(p_x c, p_y c, p_z c; E)$ transform like (x,y,z,ct) from one moving system to another. That is, if there is relative motion βc along the x axes of two systems, the primed system moving in the

plus x direction,

$$p_x' c = \frac{1}{\sqrt{1-\beta^2}} (p_x c - \beta E)$$

$$p_y' = p_y \ , \ p_x' = p_z$$

$$E' = \frac{1}{\sqrt{1-\beta^2}} (E - \beta c\, p_x)$$

and obviously $E^2 - (pc)^2 = Mc^2$ is invariant.

It is also true that in any given coordinate system the vector sum of the momenta of several particles is constant for any interactions of the particles, as is the sum of total energies The motion of an unstable particle affects its apparent lifetime. If a particle with a mean life at rest of τ_o moves with velocity $c\beta$, then its observed mean lifetime will be $\tau = \frac{\tau_o}{\sqrt{1-\beta^2}}$. The mean distance it travels before decaying is $\ell_d = c\beta\tau = \tau_o p/M$.

The different particles have different types of forces or interactions. Pions and heavier particles have "strong" or "nuclear" interactions, responsible for holding nucleons together and producing the unstable particles. Weak interactions account for beta decay of nuclei and pion-muon decay. Electromagnetic interactions occur between all electrically charged particles. Gravitational forces probably occur between all particles - certainly between nucleons - but are weak enough to be ignored for our purpose.

Electromagnetic Interactions.

The electromagnetic forces are most familiar. Classically the equation of motion is

$$\frac{d}{dt} cp = q(cE + \underset{\sim}{v} \times \underset{\sim}{B}) \quad ,$$

and in a uniform magnetic field a particle moving perpendicular to the field moves in a circle of radius

$$\rho = \frac{pc}{zeB} \text{ [cm]}$$

pc in ergs
e in esu
B in gauss.

This is more conveniently written

$$\rho = \frac{pc}{300\ zB} \text{[cm]}$$

pc in electron volts
B in gauss.

and the quantity $\frac{pc}{z}$ is denoted R and called (magnetic) rigidity. Rigidity is often expressed in units of volts.

In passing through ordinary matter particles lose energy to atomic electrons through coulomb (electrostatic) interactions. This is the dominant source of continuous energy loss by particles heavier than electrons and may be calculated from

$$\frac{dT}{dx} = \frac{4\pi e^4 z^2}{m_e c^2 \beta^2} N_o \frac{Z}{A} \left[\ln \frac{2m_e c^2 \beta^2}{I(1-\beta^2)} - \beta^2\right] \frac{ev}{g/cm^2}$$

with I = kZ, the average ionization potential, of the target material,

$$k = 11 \text{ ev}, \quad N_o = 6.02 \times 10^{23},$$

Z = atomic number of target

z = atomic number of moving particle

and the quantity in brackets is called the stopping power per electron. This expression is valid for all velocities greater than the orbital velocity of the target atomic electrons, and less than extreme relativistic velocities. In practice, electron capture and other effects change the loss rate at low velocities. Figure 2 shows proton energy loss in air.

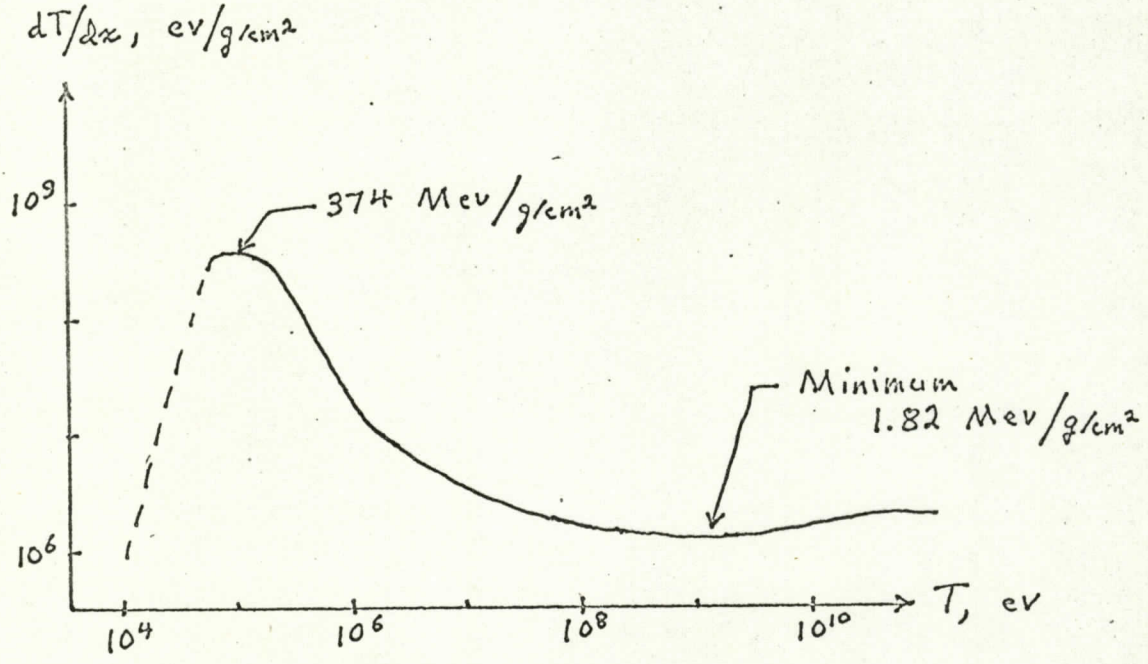

Fig. 2

Electron capture by protons becomes important when their kinetic energy drops to ~ 100 keV, and sets in at a higher energy for alpha particles.

Integration of the energy loss equation leads to a definite range as a function of initial energy, although experimental data are required for accurate work. Semi-empirically

$$R_p = 100 \left(\frac{T}{9.3}\right)^{1.8} \text{ cm of air at } 15^\circ, 760 \text{ mm Hg},$$

T in MeV.

Note that in general for any particle

$$R = \frac{M}{Z^2} F \text{ (initial velocity)}$$

The passage of a charged particle leaves a track of excited atoms (and molecules), ions, and electrons produced directly by the incident particle and by the faster electrons (δ rays). In many cases the energy per ion pair does not upon the nature of the incident particle. Some values are:

Air 34 ev/ion pair
Argon 26 ev/ion pair
Silicon 3.5 ev/hole-electron pair.

If a particle passes through a transparent target material at a velocity βc greater than the velocity c/n (n = index of refraction) of light in the material, part of the energy transferred to electrons of distant atoms appears in the special form of Cerenkov radiation instead of as ionization. This light is emitted in a cone of half angle, ϑ, about the track of the particle,

and the energy lost to it is

$$\frac{dT}{ds}_{\text{Cerenkov}} = \frac{4\pi^2 e^2 z^2}{c^2} \int_{\nu_1}^{\nu_2} \left(1 - \frac{1}{\beta^2 n^2}\right) \nu d\nu$$

$$\cos\vartheta = \frac{1}{\beta n}$$

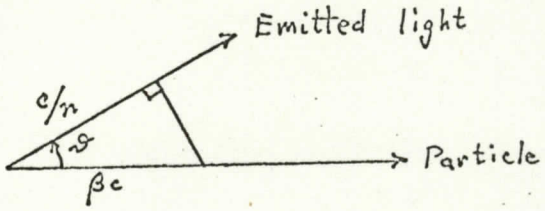

where the integration is carried out over all frequencies, ν, of the emitted light for which $\beta c > c/n$. Numerically a relativistic particle in a material such as lucite, with $\beta n \simeq 1.5$, produces 200 quanta/cm with wavelengths from 4000 to 8000 Å, and loses about 1 keV/cm. Both heavy particles and electrons produce Cerenkov light.

Electron Energy Loss

Electrons lose energy in collisions with atomic electrons as do heavier particles, although the effect is modified by the incident electron's ability to lose all its energy to a single atomic electron. The result is

$$\frac{dT}{dx}_{\text{ion}} = \frac{4\pi e^4}{m_e c^2 \beta^2} N_o \frac{Z}{A} \frac{1}{2} \left[\ln \frac{m_e c^2 \beta^2 T}{I^2 (1-\beta^2)} - \beta^2 \right] \frac{ev}{g/cm^2}$$

with T = kinetic energy.

Unlike heavier particles, electrons are scattered and also lose energy to bremsstrahlung. Elastic multiple scattering reduces the macroscopic range by a factor 1.2 to 4 below the total range, depending upon electron energy and Z of the target. Elastic

scattering cross sections are given at the end of this section.

When a particle loses energy in colliding with another particle it is said to suffer an inelastic scattering and to have lost energy to bremsstrahlung (German for stopping radiation). This energy loss is proportional to (acceleration in scattering)$^2 \propto 1/M^2$, which is why only electrons lose appreciable energy to bremsstrahlung. Because of quantum-mechanical effects only some accelerations (scatterings) produce quanta. The average rate of energy loss to bremsstrahlung by an electron of energy T in colliding with a nucleusof charge Ze is,

$$\frac{dT}{ds}_{rad} = N(T + m_e c^2)\sigma_o \bar{B} Z^2 \text{ ergs/cm.}$$

or

$$\frac{dT}{dx}_{rad} = N_o(T + m_e c^2)\sigma_o \bar{B} \frac{Z^2}{A} \text{ ergs/g/cm}^2,$$

where N = atoms/cm^3, N_o = Avogadro's number,

$$\sigma_o = \frac{e^2}{\hbar c}\left(\frac{e^2}{mc^2}\right)^2 = 0.58 \times 10^{-3} \text{ barns/nucleus; barn} = 10^{-24}\text{cm}^2.$$

$\bar{B}$ is a slowly varying function of energy as shown below:

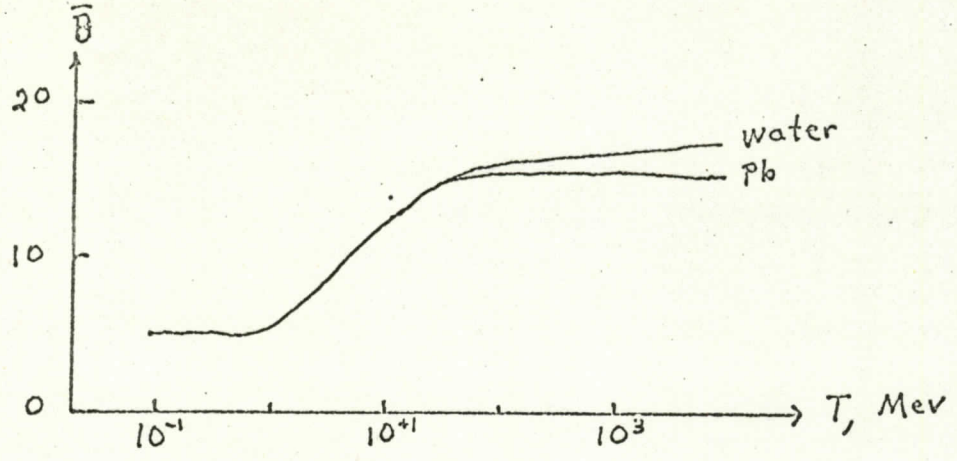

Fig. 3

Thus the rate of energy loss per g/cm^2 increases linearly with total energy and Z of the target (since Z/A ~ constant). The quantity $\sigma_o \bar{B} Z^2 = \sigma_{rad}$, the total radiative cross section.

At very high energies $\sigma_{rad} = \sigma_o Z^2 4 \left[\ell n \frac{183}{Z^{1/3}} + \frac{1}{18} \right]$.

Photons are emitted with all energies up to T, and the energy per unit frequency interval is

$$h\nu d\sigma_{rad} \text{ and } \sigma_o B Z^2 \frac{T+mc^2}{T} d(h\nu)$$

which is approximately constant since $B \simeq 10$ to 20 for $h\nu < T$. The photons are emitted perpendicular to the path of a slow electron, but more forward from a fast one.

It is convenient to compare the cross sections for the various processes. For nonrelativistic electrons we have

$$\text{Ionization } \sigma_{ion} \simeq \frac{2Z}{\beta^4} \ln \left(\frac{T\sqrt{2}}{I} \right) \text{barns/atom}$$

$$= \frac{1}{NT} \left(\frac{dT}{ds} \right)_{ion}$$

Elastic nuclear backscattering

$$\sigma_{nuc} \simeq \frac{1}{4}\frac{Z^2}{\beta^4} \text{ barns/atom}$$

Elastic scattering (>45°) from atomic electrons

$$\sigma_{elas} \simeq \frac{2Z}{\beta^4} \text{ barns/atom}$$

Bremsstrahlung in terms of fraction of kinetic energy

$$\sigma'_{rad} = \frac{T+mc^2}{T}\sigma_{rad} \simeq \frac{8}{3\pi}\frac{1}{137}\frac{Z^2}{\beta^2} \text{ barns/atom.}$$

The general form of the ionization and bremsstrahlung cross-sections (not limited to non-relativistic electrons) may be multiplied by N/density = N_o/A to give the energy loss per g/cm^2. The result is shown in Fig. 4 for energies up to 5 MeV.

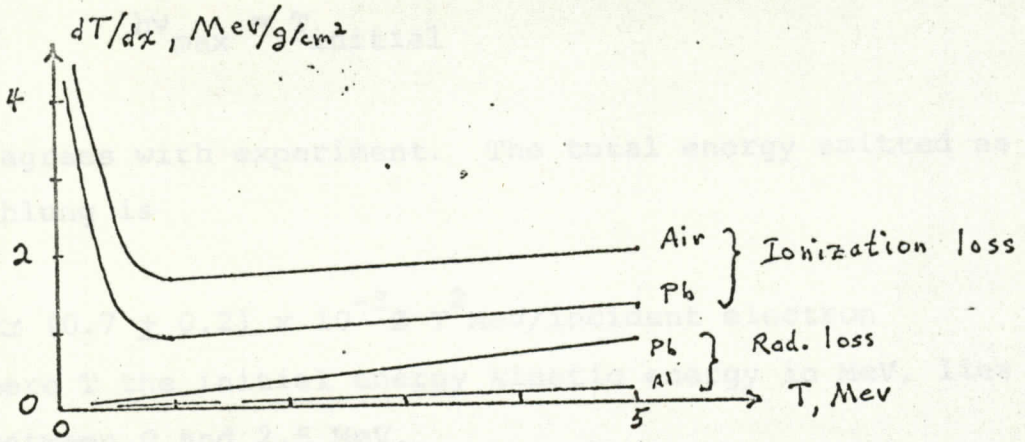

Fig. 4 Electron energy loss rate

It is useful to calculate the ratio of radiation to ionization loss. It is, for a particle of mass M

$$\frac{(dT/ds)\ \text{rad}}{(dT/ds)\ \text{ion}} \simeq Z\left(\frac{m_e}{M}\right)^2 \quad \frac{T}{1600\ m_e c^2}$$

which is unity for 9 MeV electrons in Pb, and 100 MeV in water.

The reader is cautioned that the energy loss rates in Fig. 3 cannot be integrated to give range because of scattering and fluctuations in bremsstrahlung loss. It is possible to calculate the bremsstrahlung emitted when electrons strike a thick absorber (one thick enough to stop them). The photon energy spectrum from non-relativistic electrons is

$$\frac{dI}{d\nu} = \text{const}\ Z(\nu_{max}-\nu)\ \text{ergs/frequency interval}$$

$$h\nu_{max} = T_{initial}$$

and this agrees with experiment. The total energy emitted as bremsstrahlung is

$$I \simeq (0.7 \pm 0.2) \times 10^{-3} Z\ T^2 \text{MeV/incident electron}$$

where T the initial energy kinetic energy in MeV, lies between 0 and 2.5 MeV.

The extrapolated or practical range of electrons may be

expressed by empirical formulae such as

$$R_o[mg/cm^2] = 530T-106$$

$$T = 1 \text{ to } 20 \text{ MeV.}$$

Both positrons and electrons suffer the energy losses described. In addition, positrons will annihilate with electrons, after slowing down, to yield two γ rays of energy $m_e c^2$ each, moving in opposite directions.

$$e^+ + e^- \rightarrow 2\gamma$$

Photon Energy Loss

Photons passing through matter lose most of their energy in one of three processes , the dominant one being determined by the photon energy and Z of the target material. These are:

photoelectric absorption	$E_\gamma = h\nu \lesssim$ few x 10^5 ev
Compton scattering	$\sim 0.1 \leq h\nu \leq 3$ MeV
pair production	$h\nu \gtrsim 3$ Mev

In addition the processes

photo-disentegration of nuclei, e.g. $Be^9(\gamma, n)Be^8$, $h\nu > 8$ Mev

photo-production of mesons $h\nu > 150$ Mev

are sometimes observed.

Photoelectric absorption occurs when a photon interacts with an electron bound in an atom, giving up all its energy to the electron; i.e., the photon is completely absorbed. The electron kinetic energy is

$$T = h\nu - B_e$$

B_e = binding energy of electron

The presence of the atom is necessary because the atom must carry away some momentum from the interaction. The crossection α^T cm^2/atom varies rapidly with Z and $h\nu$. When $h\nu$ is not near any electron binding energy, it is found that

$$\alpha^T = \text{const} \frac{Z^n}{(h\nu)^\gamma} \quad \text{and} \quad \begin{matrix} n = 4.0 \text{ to } 4.6 \\ \gamma = 3 \text{ to } 1 \end{matrix}$$

as $h\nu$ goes from 0.1 to 3 Mev.

Near a binding energy τ changes discontinuously (an absorption edge) as shown in Fig. 5.

In Compton scattering a photon interacts with either a bound or unbound electron, the presence of the atom being irrelevant since both momentum and energy can be conserved by a scattered photon of lower energy, and the struck electron.

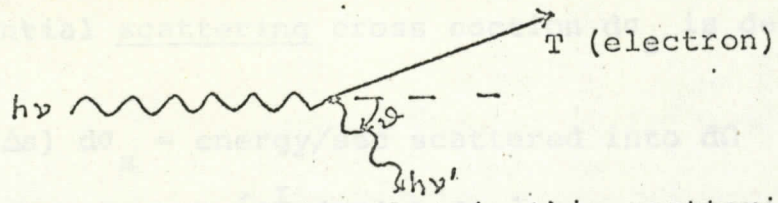

The conservation laws require that in this scattering:

Wavelength change $\lambda' - \lambda = \frac{h}{m_e c}(1 - \cos\vartheta)$

Energy change $\frac{h\nu'}{h\nu} = \frac{1}{1 + \alpha(1 - \cos\vartheta)}$, $T = h\nu - h\nu'$

with $\alpha = h\nu/m_e c^2$.

Note that the maximum energy that can be transferred to the electron is

$$T_{max} = h\nu \frac{2\alpha}{1+2\alpha}$$

The cross section for this process can be calculated from the laws of quantum-electrodynamics and the result, averaged over polarization directions of the incoming photon is:

$$d\sigma_c = \frac{r_o^2}{2}\left(\frac{\nu'}{\nu}\right)^2\left[\frac{\nu}{\nu'} + \frac{\nu'}{\nu} - \sin^2\vartheta\right]d\Omega \quad \frac{\text{cm}^2}{\text{electron}}$$

differential collision cross section

with

$$r_o = \frac{e^2}{m_e c^2} = 2.818 \times 10^{-13} \text{ cm.}$$

The meaning of this is that, if $I = \text{ev/cm}^2\text{sec}$, the energy flux of the incoming beam, then

$$\frac{I}{h\nu}(NZ\Delta s)\, d\sigma_c = (\text{number of photons/sec scattered into } d\Omega \text{ at angle } \vartheta \text{ by one cm}^2 \text{ of an absorber having } \Delta s N Z \text{ electrons/cm}^2 \text{ in a thickness } \Delta s).$$

We assume that Δs is small so that scattered photons do not suffer further interactions.

The differential scattering cross section $d\sigma_s$ is defined by

$$I(NZ\Delta s)\, d\sigma_s = \text{energy/sec scattered into } d\Omega$$
$$= h\nu' \left[\frac{I}{h\nu}(NZ\Delta s)\, d\sigma_c\right]$$

Hence

$$d\sigma_s = \frac{\nu'}{\nu}\, d\sigma_c .$$

These cross sections may be integrated over $d\Omega$, taking account of the dependence of ϑ on ν', to yield the average collision cross section, which for small α can be expressed

$$\sigma_c \simeq \frac{8\pi}{3} r_o^2 [1 - 2\alpha + 5.2\alpha^2 + \ldots] \text{ cm}^2/\text{electron}$$

$$\frac{I}{h\nu}(NZ\Delta s)\sigma_c = \text{number of photons scattered/sec}$$
$$= \text{number of electrons recoiling/sec}$$

The average scattering cross section is similarly obtained by integration, and for small α equals

$$\sigma_s \simeq \frac{8\pi}{3} r_o^2 [1 - 3\alpha + 9.4\alpha^2 + \ldots] \text{cm}^2/\text{electron}.$$

$I(NZ\Delta s)\,\sigma_s$ = energy in the form of photons scattered/sec. Hence the average energy of a scattered photon is

$$\overline{h\nu'} = \frac{\sigma_s}{\sigma_c} h\nu,$$

and the average electron energy is

$$\overline{T} = h\nu - h\nu' = h\nu(1 - \sigma_s/\sigma_c) .$$

Therefore $I\,(NZ\Delta s)(\sigma_c - \sigma_s)$ = energy going to electrons per second, and it is convenient to define the absorption cross section

$$\sigma_{abs} = \sigma_c - \sigma_s$$

(small α) $$\simeq \frac{8\pi}{3} r_o^2 [\alpha - 4.2\alpha^2 + \ldots] \text{ cm}^2/\text{electron}$$

The scattered electrons and photons are projected generally forward, the direction being more strongly peaked the greater α. Note that σ_{abs} is proportional to the energy deposited in a thin absorber, while σ_c is proportional to the number of photons removed from the incident beam. The actual reduction observed when the absorber is placed in the beam depends upon the type of detector used.

When the energy of an incident photon $h\nu > 2 m_e c^2$, it is possible for a photon to be absorbed in the coulomb field of a nucleus and create an electron-positron pair. The nucleus recoils and absorbs some momentum, but essentially no energy, so that

$$T_{e^+} + T_{e^-} = h\nu - 2 m_e c^2.$$

The distribution of energies of the e^+, say, is nearly flat from 0 to $h\nu - 2m_e c^2$, and the total crossection is

$$_a\kappa = \sigma_o Z^2 \bar{P} \text{ cm}^2/\text{nucleus}$$

where $\bar{P} \simeq 2$ to 11 for $h\nu = 5$ - 1000 Mev, and drops to zero at lower energies. For very high energies

$$\bar{P} = \left[\frac{28}{9} \ln\left(\frac{183}{Z^{1/3}}\right) - \frac{2}{27}\right].$$

These crossections may be converted to attenuation lengths in g/cm^2 as follows

$$\ell = \frac{\rho}{N\tau + NZ\sigma_c + Nk} = \frac{A}{N_o} \frac{1}{\tau + Z\sigma_c + k} \text{ g/cm}^2$$

The quantity $1/\ell$ in Pb is plotted against $h\nu$ in Fig. 5.

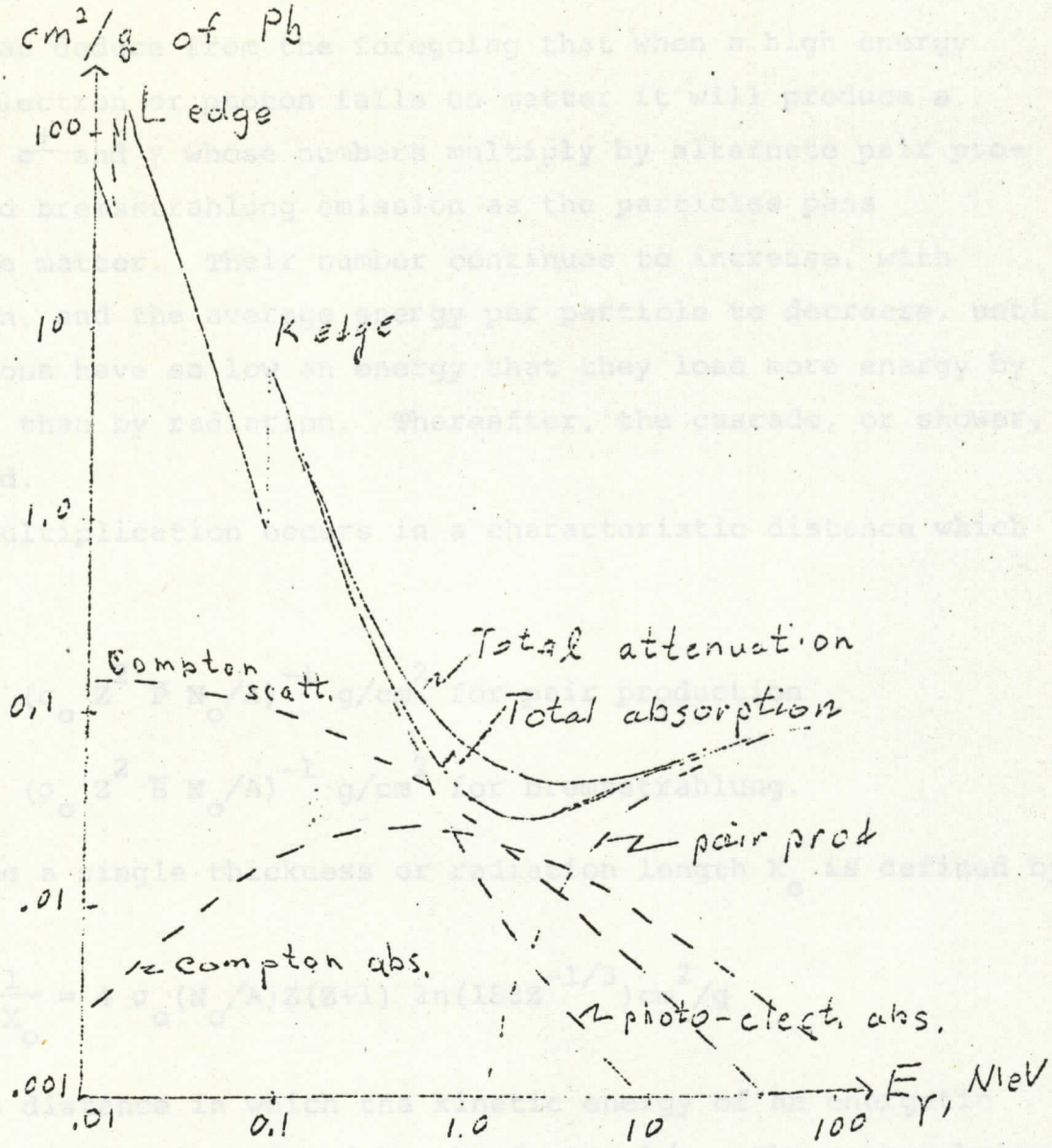

Fig. 5.

Because photons are removed catastrophically by these processes, they are attenuated exponentially in passing through matter.

Since $I/h\nu$ = photon flux we have

$$\frac{I(x)}{h\nu} = \frac{I_o}{h\nu} e^{-x/\lambda}$$

One can deduce from the foregoing that when a high energy ($\geq m_e c^2$) electron or photon falls on matter it will produce a cascade of $e^{\pm}$ and γ whose numbers multiply by alternate pair production and bremsstrahlung emission as the particles pass through the matter. Their number continues to increase, with penetration, and the average energy per particle to decrease, until the electrons have so low an energy that they lose more energy by ionization than by radiation. Thereafter, the cascade, or shower, is absorbed.

The multiplication occurs in a characteristic distance which is

$$\sim (\sigma_o Z^2 \overline{P} N_o/A)^{-1} \text{ g/cm}^2 \text{ for pair production}$$

$$\sim (\sigma_o Z^2 \overline{B} N_o/A)^{-1} \text{ g/cm}^2 \text{ for bremsstrahlung.}$$

In practice a single thickness or radiation length X_o is defined by

$$\frac{1}{X_o} = 4 \sigma_o (N_o/A) Z(Z+1) \ln(183 Z^{-1/3}) \text{cm}^2/\text{g}$$

and is the distance in which the kinetic energy of an energetic electron or photon is reduced by the factor 1/e. The energy below which multiplication is unimportant is called the critical energy T_c.

Material	X_o, g/cm^2	T_c, MeV
Air	37.7	84.2
Al	24.5	48.8
Pb	6.5	7.8

If the initial particle has energy T_o, then after traversing a

thickness x g/cm^2 there are $\sim 2^{x/(X_o \ell n 2)}$ particles (1/3 γ, 2/3 $e^{\pm}$) of average energy $T_x = T_o/2^{x/(X_o \ell n 2)}$. The maximum number of particles occurs when $T_x = T_c$, and is equal to T_o/T_c. Detailed calculations have been made of both the longitudinal and lateral spread of these showers in the atmosphere.

Weak Interactions

The weak interaction forces couple the initial and final particles in beta decay, exemplified by pion, muon, and neutron decay, and by the interaction of neutrinos with matter. These forces always involve some particles which do not experience nuclear interactions; i.e., electrons, muons, neutrinos.

Neutrinos carry away, as kinetic energy, a significant amount of the energy released in beta decay. Once produced, they interact very weakly with matter. The interaction cross section $\sigma_\nu = 10^{-44}$ cm^2/nucleon, so that the mean free path of neutrinos in Fe is 10^{22} g/cm^2 or 1000 light years of solid iron. Therefore the energy going into neutrinos is lost from the vicinity of the neutrino's production. This is certainly true in the case of neutrinos produced by cosmic ray interactions in the atmosphere, and neutrinos escape even from the interiors of stars, carrying an appreciable amount of the energy produced there with them. However, stellar material is very dense, and it is a current subject of theoretical research to calculate how many neutrinos escape from various kinds of stars. Experiments are also underway to measure the flux of extraterrestrial neutrinos by observing the rate of the reaction

$$\nu + C\ell^{37} \rightarrow A^{37} + e^-$$

which is the inverse of the electron capture decay of A^{37} to Cl^{37} (35 day half life). In practice large tanks (thousands of gallons) of C_2Cl_4 (cleaning fluid) are shielded from charged particles, and any A^{37} produced is flushed out with other gases. The A^{37} disintegrations are then counted with a small Geiger counter.

Muon decay goes as

$$\mu^{\pm} \rightarrow e^{\pm} + \nu + \bar{\nu} + 105.2 \text{ MeV}$$

the kinematics of three body interaction allowing electron energies 0 - 53 MeV in the center of mass system. Most cosmic ray secondary muons decay in flight after travelling a considerable distance. For example, for a 10.3 BeV muon

$$\tau(\beta) = 2.16 \times 10^{-4} \text{ sec},$$
$$\ell_d = 65.0 \text{ km},$$

which is greater than the height of most of the atmosphere. Some muons are stopped by ionization loss and decay at rest. Negative muons are usually captured into Bohr orbits around a nucleus, and because of their large mass spend much time inside the nucleus. On the average a μ^- passes through 10^{17} g/cm^2 of nuclear matter without interacting, but occasionally the weak interaction

$$\mu^- + p \rightarrow n + \nu$$

occurs. This is the inverse of neutron decay.

Charged pions decay according to the scheme

$$\pi^{\pm} \rightarrow \mu^{\pm} + \nu + 33.9 \text{ MeV}$$

and the two body decay fixes the muon energy at 4.1 MeV in the CM system. For a 13 BeV pion

$$\tau(\beta) = 2.4 \times 10^{-6} \text{ sec},$$
$$\ell_d(\beta) = 712 \text{ meters}.$$

Pions rarely stop before they decay. They suffer nuclear interaction with about the same probability as nucleons, and so an energetic charged pion may well have a nuclear interaction before decaying.

Neutral pions decay into two γrays so rapidly that nuclear interactions are unlikely.

$$\pi^o \rightarrow 2\,\gamma + 135.1 \text{ Mev.}$$

At 13 Bev, a π^o has

$$\tau(\beta) = 1.44 \times 10^{-13}$$

$$\ell_d(\beta) = 4.3 \times 10^{-3} \text{cm.}$$

Strong Interactions

The pions and all heavier particles interact with strong, i.e., nuclear, forces, which are essentially independent of electric charge except that at low energies Coulomb repulsion may prevent particles coming close enough to interact. At energies the order of or less than the binding energy of nucleons in nuclei (8 Mev) nuclear reactions are extremely complex. At higher energies it is a pretty good approximation to assume that nucleons and nuclei interact if they come within a fixed distance, about equal to the sum of their classical radii ($R = 1.2 \times 10^{-13}\ A^{1/3}$) of each other, and otherwise not at all. Hence the crossection for interaction between a pion or nucleon and a nucleus of weight A is

$$\sigma_{nuc} = 0.05\ A^{2/3} \text{ barns/nucleus,}$$

and the mean free path for nuclear interaction is

$$\ell_{nuc} \simeq 33\ A^{1/3}\ \text{g/cm}^2.$$

What happens depends upon the kinetic energy of the collision. If the kinetic energy of the incident particle merely divides among the kinetic energies of the incident and target particles the collision is elastic. In order for mesons to be created, the kinetic energy of the initial particles in the CM (center of mass or zero momentum) system must equal or exceed the rest mass energy of the mesons created. Thus the reaction

$$p + p \rightarrow p + n + \pi^+$$

requires $T_p \geq 293$ Mev in the lab system. If the target nucleon is

bound in a nucleus, it has some kinetic energy of motion, and the required incident energy is somewhat less.

The probability of meson production increases slowly with increasing energy, but the inelasticity, defined as the fraction of kinetic energy in the CM system used for meson creation, does not equal 1/2 until T_p = 1.7 Bev. With further increases of energy, the number of mesons increases slowly and the average energy per meson increases.

When an energetic particle strikes a C, N, or O nucleus of the atmosphere, or a Ag or Br nucleus in a photographic emulsion, particles emerge with various velocities, and these are categorized according to the density of the ionization tracks they make in the surrounding medium. (Grain density in an emulsion.)

shower particles (thin tracks)	ionization <1.41 times minimum	E_p> 80 Mev E_π> 500 Mev
grey particles	ionization: 1.4 to 8 times minimum	80> E_p >25 Mev 500 Mev> E_π
black particles	ionization > 8 times minimum	25 Mev> E_p 800 Mev> E_α

It is found that about 80% of the shower particles are pions and the rest fast protons; the number of shower particles is denoted n_s. The total number of grey and black particles is denoted N_h. The shower particles are projected forward in the direction of the incident particle, and are produced by multiple interactions of the incident particle and shower particles with nucleons inside the struck nucleus. The grey particles diverge more from the incident direction, while the black particles are emitted isotropically. The latter are "boiled off" from the struck nucleus as the energy left in the nucleus after the passage of the intra-nuclear cascade is shared among the remaining nucleons. They are sometimes called evaporation particles.

Figure 5 shows the appearance of a nuclear star in an emulsion, and Fig. 6 gives values of n_s and N_h produced by cosmic rays and machine accelerated protons in an emulsion

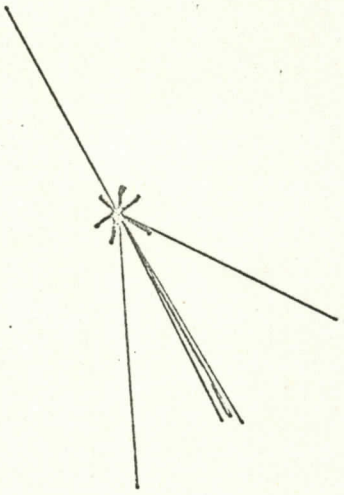

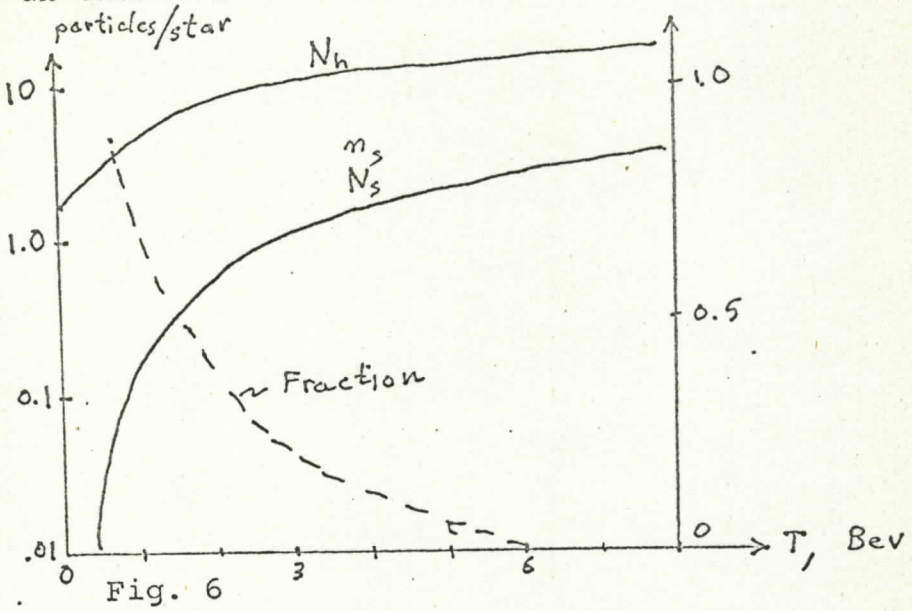

Fig. 6

Note that π^+, π^-, π^0 are produced in about equal numbers at the same energies as are p^+ and n^0, but that the neutral particles make no tracks.

References

Evans, R. D., The Atomic Nucleus, McGraw Hill, New York 1955

Rossi, B., High Energy Particles, Prentice Hall, New York 1952

Leighton, R. B., Principles of Modern Physics, McGraw-Hill, New York, 1959.

Rich and Madey, Range Energy Tables, UCRL-2301

Whaling, W., "The Energy Loss of Charged Particles in Matter", Handbuch der Physik 34, Springer Verlag

19.4 Interactions of Cosmic-rays in the atmosphere

The processes described in 19.3 cause a very complex chain of interactions when a high energy cosmic ray nucleus enters the atmosphere (or other extended material) and collides with a nucleus. Figure 7 shows these schematically. The trajectories are spread for clarity; in fact the primary and energetic secondary particles move almost colinearly.

The intensity and energy spectrum of each type of secondary radiation varies with atmospheric depth, with zenith angle of the direction of motion, and with geomagnetic latitude. An exact calculation can be made of the production and loss rates of each type of radiation from each energy interval, and it is found that the experimental data can be fitted reasonably well. The most important features of the secondary production are summarized in Fig. 8 which is drawn for a mid-latitude when the cutoff is 2 Bev. They can be accounted for as follows:

The nucleonic component (nucleons with E > 1 Bev) can be thought of as the source of the other radiations. These interact with a mean free path of ~ 65 g/cm^2, and in each interaction an average of 2.7 shower particles is produced, of which 20% are fast protons and the remainder pions.

Thence the change in the flux N of the nucleonic component in passing through a thickness dx is

$$dN = N\,dx\left(-\frac{1}{L}+\frac{2.7 \times 0.2}{L}\right)$$

or

$$N = N_o\, e^{-x/L_{abs}}$$

of which half are protons and half neutrons.

L = 65 g/cm^2 observed

L_{abs} = 145 g/cm^2 calculated.

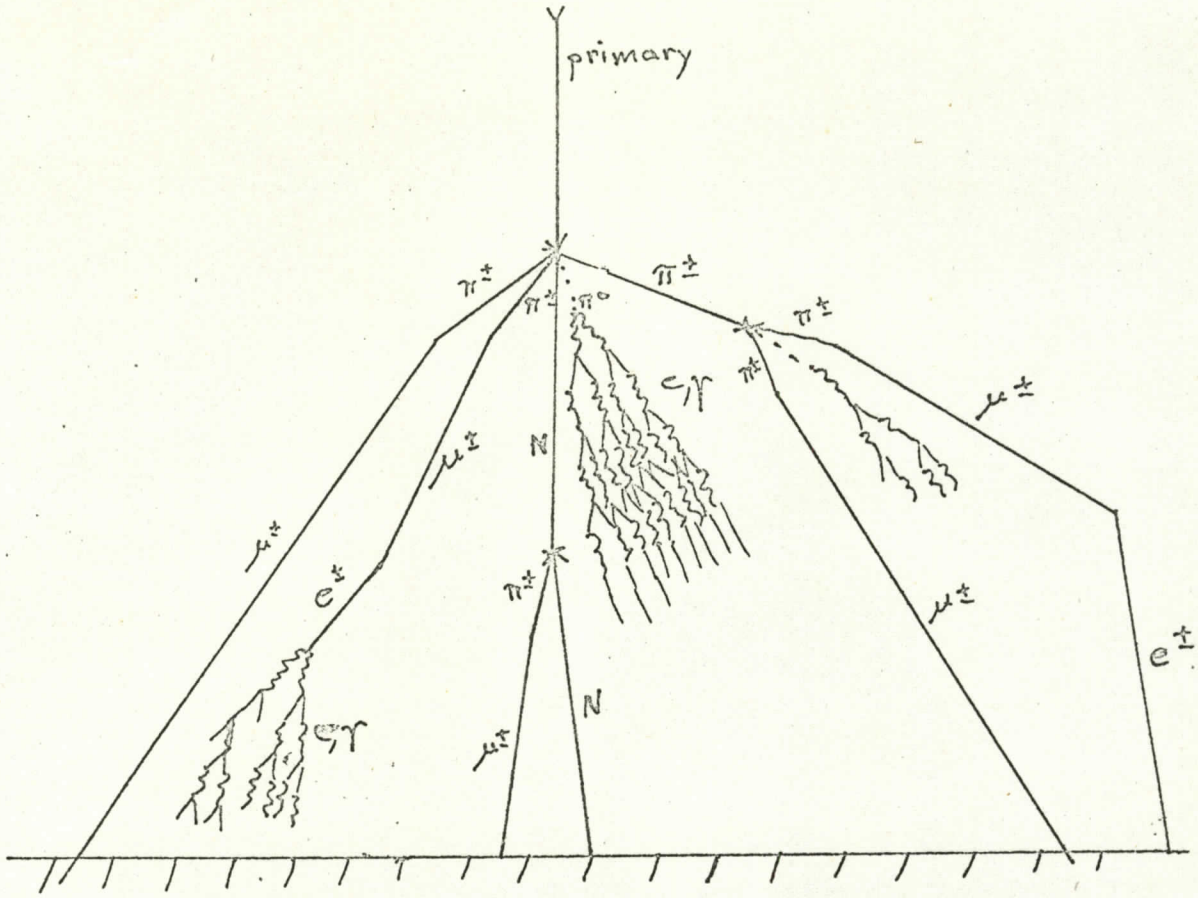
primary
$\pi^\pm$
$\pi^\pm$
$\pi^\pm$
$\pi^\pm$
$\pi^\pm$
π^0
$\pi^\pm$
$\pi^\pm$
$\mu^\pm$
$\mu^\pm$
$\mu^\pm$
$\mu^\pm$
$\mu^\pm$
$e^\pm$
$e^\pm$
$e\gamma$
$e\gamma$
N
N
N

Fig. 7

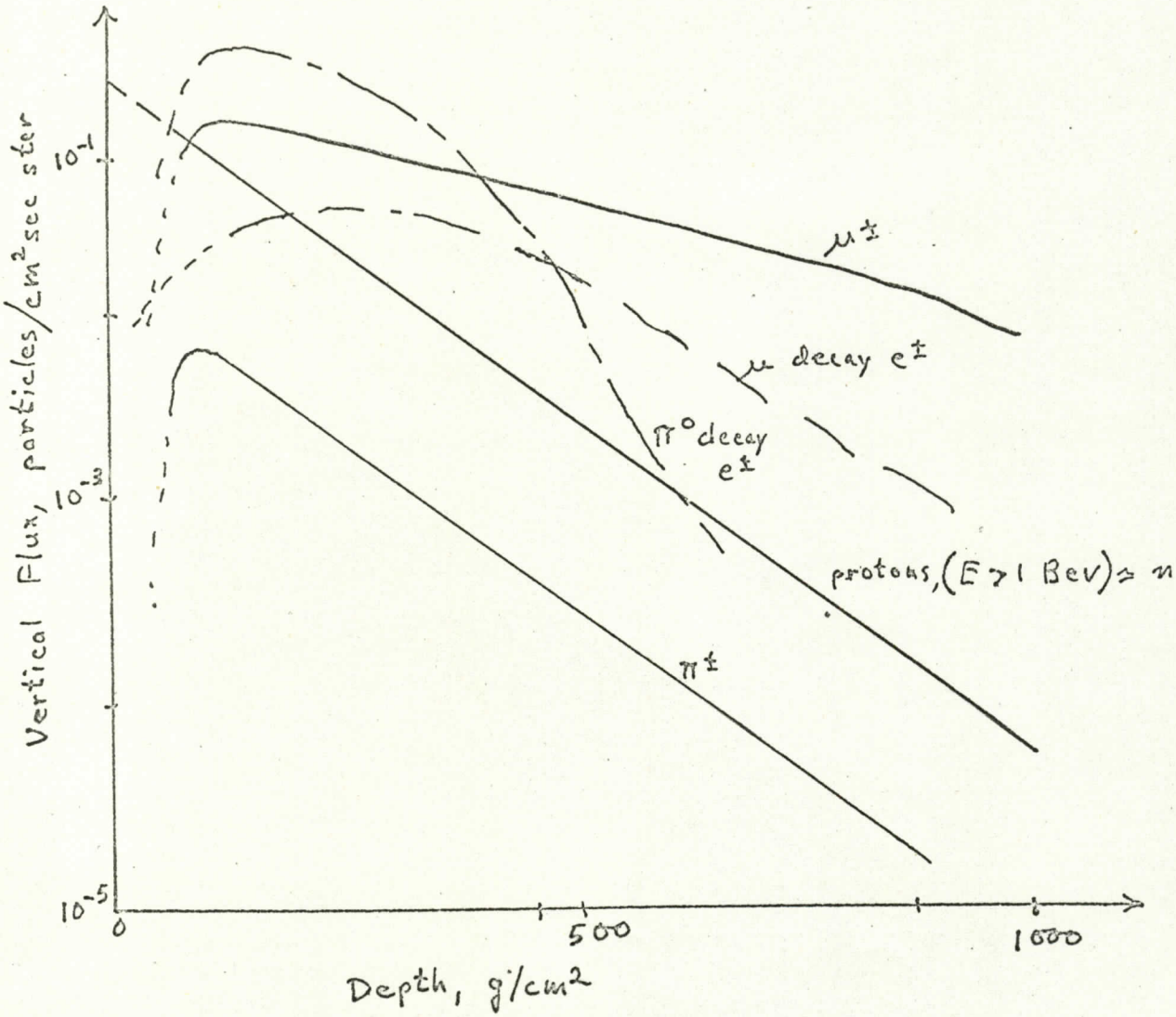
Vertical Flux, particles/cm² sec ster
10⁻¹
10⁻³
10⁻⁵
0
500
1000
Depth, g/cm²
μ±
μ decay e±
π° decay e±
protons, (E > 1 Bev) ≈ n
π±

Fig 8

Actually the observed exponential absorption length of the nucleonic component is ~ 125 - 140 g/cm^2. Since the above approximation has neglected neutron production and loss of secondary nucleons below the (arbitrary) threshold of 1 Bev, the agreement is very satisfactory.

The production rate of evaporation particles and slow neutrons in nuclear stars is proportional to the nucleonic component, and because the slow particles have a range ~ 0.1 g/cm^2 their flux is isotropic and proportional to the total nucleonic component integrated over angle. If this total flux is N_{tot}, then

$$\text{Flux of evaporation particles} \simeq N_{tot}\left(\frac{\text{range of evaporation particles}}{L}\right)$$

$$\simeq N_{tot}\ \frac{0.1}{65}\ .$$

Pions produced in nuclear collisions decay after traveling an average distance of ℓ_d ~ 200 meters (E_π = 3.7 Bev) which at sealevel is only 26 g/cm^2. These suffer collisions like the nucleonic component, but clearly throughout most of the atmosphere most pions decay before interacting. Hence from 50 to 500 g/cm^2 the pion flux, π, is approximately

$$\pi = N\ \ell_d\ \rho\ \frac{2.2}{L}$$

with the density $\rho = X/H$

and X = g/cm^2 depth in the atmosphere

H = 8 km, the scale height.

numerically $\pi = \frac{NX}{1200}$, but the rise with increasing depth

is partially offset by the increasing probability that pions interact before they decay.

In contrast with pions, the average muon travels an appreciable fraction of the atmosphere before decaying so that their number decreases more gradually. Decaying muons are a source of fast electrons, and the dominant one at depths greater than ~ 600 g/cm^2. Higher in the atmosphere, electrons from π^o initiated electronic cascades predominate. These electrons are actually half positrons, and half negative electrons; the number of cascade photons equals the number of negative electrons. The data in Fig. 8 refers to electrons above the critical energy.

The fluxes of primaries and secondaries varies somewhat with latitude. At lower latitudes, where the minimum rigidity able to reach the top of the atmosphere is greater, the fluxes are less than shown, the change being greatest at high altitudes, and the maximum (call Pfotzer or transition maximum) moves to a lower altitude. In going to higher latitudes the fluxes increase to a point, called the latitude knee, and then are constant poleward because the additional primaries allowed in are of such low energy that they stop through collision loss before interacting. In the polar cap region the total flux of nucleons (primaries) may increase rapidly from ~ 50 g/cm^2 depth to the top of the atmosphere.

It is of interest to note an older classification of radiation based on range. This is

Hard component (Range > 10 to 18 cm of Pb)

Protons, $E_p > 0.5$ Bev

Muons, $E_\mu > 0.25$ Bev

Soft component (Range < 10 to 18 cm of Pb)

Electrons

Muons, $E_\mu < 0.25$ Bev

Slow nucleons $E < 0.5$ Bev.

In oblique directions (zenith angle $\zeta > 0$) a first approximation is that the flux of particles at a depth X is equal to the vertical flux at a depth $x/\cos\zeta$. This assumes that all secondaries move colinearly with their generating primary, and neglects the fact that decay depends upon distance traveled, not upon mass transversed; it is called the Gross approximation.

19.4.1 At present the secondary radiation is of interest principally because experiments that measure the intensity of primary radiation by means of detectors at the surface of the earth or at balloon altitudes respond in part or altogether to the secondary radiation. At sealevel the radiation intensities in a vertical direction are:

muons .008/cm^2 sec ster

electrons .003/cm^2 sec ster

mucleons .0001/cm^2 sec ster

The muon flux depends upon the total mass of air overhead, i.e., the barometric pressure, and upon the spatial extent of the atmosphere, i.e. the temperature distribution, through the probability of pion and meson decay. The coefficients are

-0.18% per ^oK

-3.45% per cmHg

Neutron monitors have been devised which respond only to the flux of nucleons by counting neutrons produced locally by the fast

nucleons in material surrounding slow neutron counters. These monitors respond to primaries of lower average energy ($E>2$ Bev) than do meson monitors ($E \geq 20$ Bev) and have the advantage that the nucleon flux depends primarily on barometric pressure and very weakly upon atmospheric temperature.

Variations of higher energy primaries have been studied by measuring the meson component underground. Energetic mesons ($E > 2 \times 10^7$ MeV) are found as deep as 1000 meters of water equivalent (10^5 g/cm^2) underground, where the flux is $\sim 10^{-4}$ that at sealevel.

The flux of primaries with $E > 10^{15}$ ev can be deduced from observations of extensive air showers (EAS). In this technique the electrons resulting from an energetic electronic cascade are detected by an array of fast counters (usually large scintillators) spread out on the earth. By measuring the energy loss in each counter in coincidence, and the delay time between arrival of the particles at the various counters it is possible to deduce the number electrons in the shower and the direction of arrival of the particles, which propagate through the atmosphere in a thin disc. Hence it is possible to deduce the primary cosmic-ray's energy and direction. The electron flux falls off in a calculable way from a maximum on the shower axis. It is found that most large showers have multiple cores,-local-peaks of intensity in a plane perpendicular to the axis,--which probably come from the decay of several π^o produced in one or more nuclear interactions. Some showers have single cores, and it is hypothesized that these may result from primary electrons or gamma rays.

The largest EAS array in operation is at Volcano Ranch, New Mexico, and is 1800 meters across. It records ~ 2×10^4 showers per year of more than 10^7 electrons each.

19.4.2 The flux of secondary particles projected upward from the top of the atmosphere, called splash albedo, is of special interest for balloon borne experiments for which it often constitutes an unwanted background. Charged splash albedo with magnetic rigidity less than the magnetic cutoff rigidity at the point it leaves the atmosphere is returned by the geomagnetic field to the same latitude in one hemisphere or the other , and is called reëntrant albedo. In various experiments these fluxes have been measured:

At geomagnetic latitude, $\lambda_m = 55^\circ$

Vertical, fast splash albedo = $.0084/cm^2$ sec ster

At $\lambda_m = 41^\circ$, more recent, complete measurements have shown

Vertical splash albedo

Protons 90-350 Mev = 5 to 15% of primary flux

$\simeq .02/cm^2$ sec ster

Electrons 10-500 Mev = primary flux

$\simeq 0.2/cm^2$ sec ster

Measured reentrant albedo flux equaled the splash flux

Neutrons 1-14 MeV = $0.24/cm^2$ sec

Thermal neutron density < $10^{-7}/cm^3$

Neutrons of less than 0.66 ev are gravitationally trapped. Decaying energetic neutrons are one source of the inner Van Allen belt protons.

19.4.3 It is sometimes useful to summarize the interactions of cosmic-rays in the atmosphere by calculating the energy balance of the radiation. At mid-latitudes this is

Lost to ionization	64%
Lot to neutrinos	24%
Overcoming binding energy of nuclei	8%
Flux into earth	4%

Although most of the collision loss is incurred by charged particles transferring energy to atomic electrons, there is some loss in elastic scattering of fast neutrons on atmospheric nuclei. Neutron production is of special interest, and is considered at length in the following paragraphs.

19.4.4 Free neutrons are produced throughout the atmosphere in nuclear collisions. About 90% are liberated by evaporation from nuclear stars with an average energy of 1 MeV; the remainder are knocked out of nuclei with higher energies. The total production peaks at an atmospheric depth of ~ 100 g/cm^2 and declines exponentially at depths >200 g/cm^2 with an e-folding length of 160-200 g/cm^2 at $\lambda_m = 50^o - 0^o$.

Most of these neutrons are thermalized by elastic collisions with air nuclei before they decay or are lost from the atmosphere. Typically a 2 MeV neutron diffuses 50 g/cm^2 vertically and makes 134 collisions in dropping from 2 MeV to 0.1 ev. The resulting differential energy spectrum varies as 1/v with T = 0.1 ev to 10 MeV; the differential spectrum decreases at still lower energies, primarily because N^{14} in the atmosphere absorbs thermal neutrons (T < 0.1 ev) with a cross section proportional to 1/v. The density of thermal neutrons, and therefore of N^{14} absorption, has a maximum at ~ 100 g/cm^2 depth and is nearly two orders of magnitude less at sealevel. The principal capture reactions are

$$N^{14} + \quad \rightarrow \quad C^{14} + H^1 \quad .$$

$$N^{14} + n \rightarrow \quad C^{12} + H^3 \qquad \text{10\% of } C^{14} \text{ production.}$$

19.5 Several of the nuclides produced by cosmic rays in the atomsphere are of interest, but we will limit our discussion to C^{14}. Radio carbon decays according to the scheme

$$C^{14} \rightarrow N^{14} + e^- + \nu + 0.158 \text{ MeV}$$

with a half life of 5568 years. (A more recent value is 5730 yr.)

Most C^{14}, therefore, is oxidized to CO_2 and then thoroughly mixed from the stratosphere, where it is produced, into the other reservoirs listed in Table III.

TABLE III. Reservoirs of Carbon

Reservoir	Mixing time	Total stored carbon per cm^2 of earth's surface
Stratosphere	1- 8 years	0.126 g/cm^2
Troposphere	30-90 days	
Water vapor	4-14 days	
Biosphere plus humus	(30 yr, est.)	0.275
Surface ocean plus marine biosphere	20 years	0.151
Deep ocean plus	500-3000 years	$\frac{7.328}{7.88\ g/cm^2} = C_{tot}$.

Earlier estimates gave a total of 8.3 g/cm^2
The total amount of C^{14} is about 10.6×10^{-12} g/cm^2

If the rate of production of C^{14} per cm^2 of the earth q atoms/sec cm^2, is constant for several half-lives, then the disintegration rate per cm^2 must equal q. The number of C^{14} disintegrations per second per gram of total carbon therefore equals $q/C_{tot} = r_o$, and this ratio will apply to living organisms as well as all other reservoirs. However, after an organism dies it no longer exchanges C^{14} with the other reservoirs, if it is preserved intact, and the C^{14} disintegration rate per

gram, r, declines with time like

$$r = r_o e^{-(t-t_o)/\tau}$$

where τ_o is the time at which death occurred. By measuring r, therefore, it is possible to determine when an organism died. The latter date is often assumed to be the time when wood was incorporated into an artifact or structure, etc.

A global average value of $q = 2.5/cm^2 sec$ has been calculated from estimates of the neutron balance per cm^2 of the earth's surface based on neutron measurements in the atmosphere:

	n Source	C^{14}	Leakage	other n capture
Solar max.	3.22	2.08	0.29	0.85
Solar min.	4.10	2.61	0.41	1.08

However, an earlier calculation, gives $q = 1.8 \pm .3$. A value of q can be obtained from measurements of r_o and knowledge of C_{tot} if it is assumed that q has been constant. A value $q \simeq 1.9$ disintegration/ $cm^2 sec$ is obtained in this way.

In order to determine if q has been constant the ages of historically datable objects and of samples from tree rings are dated by the C^{14} method. In general the C^{14} age is somewhat less, as if q had been greater in the past than its present value. Yet the present value of q calculated from the present value of r_o is less than the present estimate of q based on neutron measurements.

The ratio r_o can be temporarily changed if climatic changes alter the amount of CO_2 in the atmosphere. Recent injection of C^{14} into the atmosphere by bomb testing has further confused interpretation of data.

19.6 The variation of cosmic ray intensity with geomagnetic latitude is caused by the fact that the geomagnetic field prevents charged particles with less than a minimum rigidity, R_c, (cutoff rigidity) reaching a given location moving in a given direction if the particles start infinitely far from earth. In general all higher rigidities are allowed. The value of R_c depends upon both location and direction of arrival, and varies roughly from 15 Bv to 0 at latitudes from 0 to 90^o.

Liouville's theorem that the density of particles in phase space is constant if the motion is describable by Hamilton's (classical) equations, may be applied to motion in a static magnetic field. In this case it implies that the directional intensity, j particles/cm^2 sec ster, of particles with energy in dE along a particle orbit is constant. Thence if the flux of charged particles with energy in dE is uniform and isotropic far from the earth, and if these particles are able to reach a given location within the geomagnetic field at all, they do so with the same energy and directional intensity, j, as they have infinitely far away.

Thus, the total flux that arrives at a given location from a given direction equals the integral flux at infinity of all particles with rigidities > R_c of the location in question.

The geomagnetic field resembles a dipole sufficiently enough that calculation of R_c is usually made by computing R_c for a dipole and then correcting this first approximation for various non-dipole perturbations. The theory of motion in a dipole field was first

developed by Stormer, and elaborated by Lemaître and Vallarta.

The equations of motion are

$$\frac{d}{dt}\underset{\sim}{p} = \frac{Ze}{c}\underset{\sim}{v} \times \underset{\sim}{B}, \qquad \underset{\sim}{B} = -\mu\underset{\sim}{\chi}\frac{\cos\theta}{r^2} \qquad 19.6\text{-}1$$

where $M = 8.06 \times 10^{25}$ gauss cm^3

θ = colatitude measured from north pole

Since $|\underset{\sim}{p}|$ = constant, the equation can be written

$$\frac{d}{dt}\frac{\underset{\sim}{v}}{v} = \frac{Ze}{pc} M \underset{\sim}{\chi} \times \underset{\sim}{B}$$

Let $ds = vdt$ be the element of arc length along the particle's trajectory, and define a unit of length C_{St}, called the Störmer length, by

$$C_{St}^2 = \frac{Ze}{pc} M \text{ or } C_{St}^2 = \frac{300\ Z}{pc} M \qquad 19.6\text{-}2$$

when pc is expressed in electron volts. Then if all lengths are expressed in units of C_{st}, the equation of motion for any charged particle is

$$\frac{d^2}{ds^2}\underset{\sim}{r} = \pm\left(\frac{d}{ds}\underset{\sim}{r}\right) \times \frac{1}{r^3}\left(-\hat{r}\ 2\cos\theta - \hat{\theta}\ \sin\theta\right), \qquad 19.6\text{-}3$$

$\pm$ = sign of charge.

This cannot be integrated in terms of known functions, except in special cases such as motion in the equatorial plane, $\theta = \pi/2$.

Planar motion can be expressed in terms of eliptic functions, and there is a circular orbit at r = 1 [Störmer]. Energies of circular motion at two different distances from the earth's dipole are:

C_{St}	Pe/Z	T_{proton}
6378km	59.6 BeV	59.6 BeV
10 x 6378	0.596 BeV	190 MeV

Positive particles move from east to west.

In general the equation of motion can be separated to describe motion in a meridian plane, and motion of the meridian plane about the dipole axis. Let w, z be rectangular coordinates in a moving meridian plane which contains the particle, and φ the azimuthal angle of the meridian plane measured from some reference axis.

$$w = r \sin\theta = r \cos\lambda \qquad \lambda = \text{latitude}$$

$$z = r \cos\theta = r \sin\lambda$$

Then

$$\frac{d}{ds}\varphi \equiv \varphi' = \frac{2\gamma}{w^2} + \frac{1}{r^3}$$

where γ is a second constant of the motion, related to the impact parameter. (The first constant is kinetic energy.)

Define $$Q = w'^2 + z'^2 = 1 - (w\varphi')^2 = 1 - \left(\frac{2\gamma}{w} + \frac{w}{r^3}\right)^2$$

Then $$z'' = \frac{1}{2}\frac{\partial}{\partial z} Q$$

$$w'' = \frac{1}{2}\frac{\partial}{\partial w} Q$$

The latter pair of equations will not be used here. However, a great deal of information can be extracted from the Q equation by noting that if α = angle between the trajectory and a normal to the meridian plane ($\alpha = 0$ for W to E motion) then

$$Q = 1 - \cos^2\alpha = \sin^2\alpha$$

Obviously regions in which $Q < 0$ are forbidden, and the boundaries of these regions, $Q = 0$, are turning points of the motion where $\alpha = 0$ or π. The boundaries of the totally forbidden regions, therefore, are obtained by setting $\cos\alpha = +1$ and -1, and solving the equation

$$\cos\alpha = \frac{2\gamma}{r\cos\lambda} + \frac{r\cos\lambda}{r^3} \qquad 19.4\text{-}4$$

for r as a function of λ, with γ taking on various values. Figure 9 shows the result, and in Fig. 10 are drawn some orbits in the equatorial plane for various values of γ. It is evident that $|2\gamma|$ equals the impact parameter; i.e., the perpdendicular distance between the asympotic velocity vector and the dipole axis.

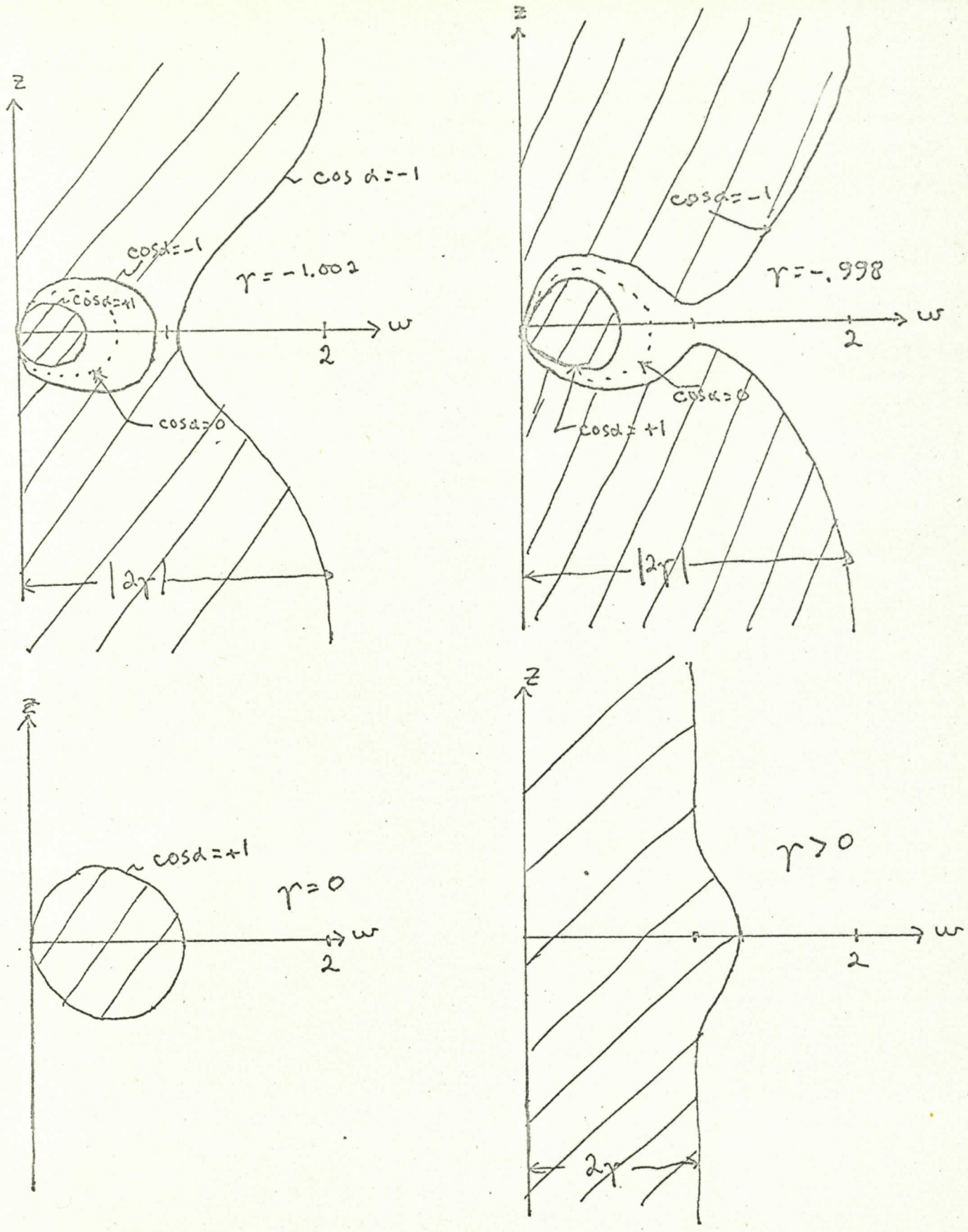

Fig 9. Meridian plane forbidden regions.

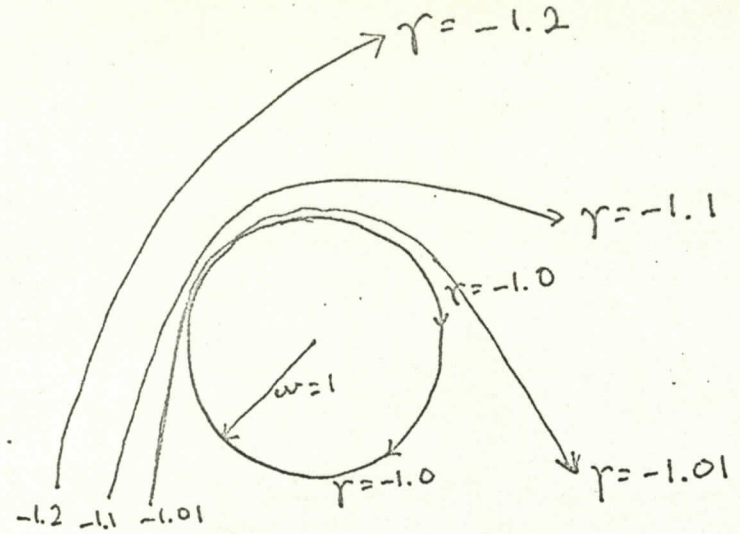

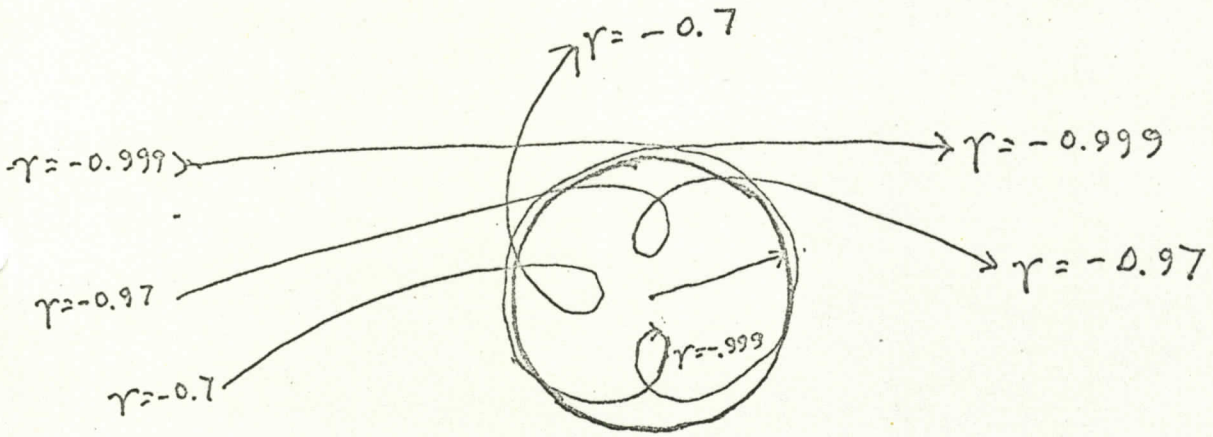

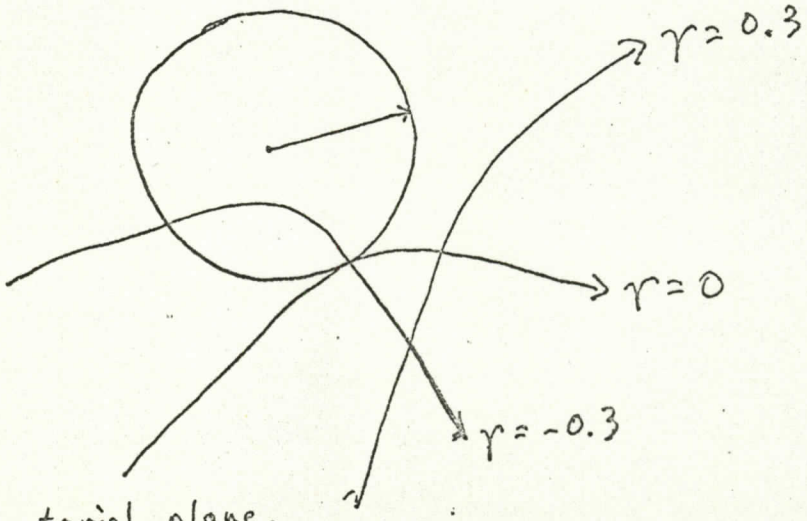

Fig 10. Orbits in the equatorial plane.

Now in the case of radiation that is isotropic and homogeneous at infinity, such as cosmic radiation, orbits with all values of γ occur. The problem of finding the cutoff rigidity at a given latitude and direction on the earth's surface is therefore reduced to finding the γ for which orbits reach a minimum distance from the dipole at the given λ and the value of α corresponding to the given direction of approach. For all λ and α this occurs when the "jaws" of the outer forbidden region have just opened and the inner forbidden region has a minimum extent.

This happens when $\gamma = -1 + \epsilon$, $1 >> \epsilon > 0$. Hence the minimum value of r is found from Eq. 19.6-4 with $\gamma = -1$. The result is

$$\frac{1}{r_{min}} = \frac{1}{\cos^2\lambda}\left(1 \pm \sqrt{1 + \cos^3\lambda \cos\alpha}\right) \qquad 19.6\text{-}5$$

with the positive root required to make r a minimum. For the earth, $r_{min}\ C_{st} = r_e = 6378$ km. Substitution into 9.6-2 gives

$$\left(\frac{r_{min}}{r_e}\right)^2 300\ M = R_{min} = \frac{59.6\ \cos^4\lambda}{\left(1 + \sqrt{1 + \cos^3\lambda\cos\alpha}\right)^2}\ \text{BeV} \qquad 19.6\text{-}6$$

Thus, the cutoff rigidity decreases to zero as $|\lambda| \to \pi/2$, and at every λ, has a maximum for positive particles arriving from the east ($\alpha=\pi$) and a minimum for those coming from the west ($\alpha=0$). The cutoff for vertical arrival is

$$R_m = \frac{59.6}{4}\cos^4\lambda\ .$$

The cone of constant α corresponding to a particular R_m and λ is called the Störmer cone. The cone may be represented by an orthogonal projection of its intersection with a unit sphere upon a horizontal plane (tangent to Earth's surface). All directions east of the Stormer cone are strictly forbidden to positive particles with $R < R_{min}$, but not all directions to the west are necessarily allowed. This is the case because for every γ such that $-1 < \gamma - .78856$, there are periodic orbits in the vicinity of the jaws. Consider a negative particle projected outward from the earth, which must follow the same orbit as a positive particle moving inward from infinity. For every λ there are directions asymptotic to periodic orbits (considering negative particles projected outward) without being reentrant, and this set of directions is called the main cone. To the east of this are directions whose orbits (called reentrant) approach the periodic orbit, then return to regions nearer the dipole, move outward again, and after repeating this one or more times are asymptotic to a periodic orbit. All such directions are forbidden to particles from infinity, but they form a set of measure zero, i.e., subtend infinitely small solid angle. However, to the east of the cones of asymptotic orbits are directions whose orbits are reentrant one or more times before escaping between the jaws to infinity. These directions are allowed, but in the presence of the solid earth one of the reentrant orbits may intersect the earth so that the directions are shadowed. Such directions are called penumbral . In addition to these penumbral directions there are directions with small elevation above the horizon for which an upward projected particle intersects the earth in its first loop about

the earth's magnetic field as shown in Fig. 11. These directions are called simple shadow cones. Figure 12 shows the complete set of cones at two latitudes

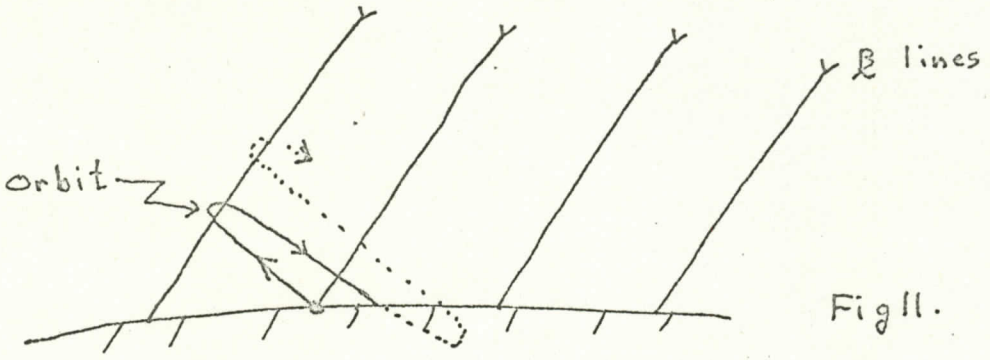

Fig 11.

Near the equator, the penumbra is nearly opaque. At higher latitudes it becomes less so. The simple shadow cones do not subtend much solid angle at any latitude.

19.6.1 Very exact calculation of Stormer orbits may not be very useful because the geomagnetic field deviates from a dipole field. At geomagnetic latitudes $\lambda \leq 55^{o}$ these deviations can be pretty well accounted for by using the eccentric dipole, or further by calculating the Störmer cutoff that would be produced by a dipole located at Earth's center, or at the eccentric dipole location, but having the strength and direction required to produce the actual surface field at the point in question. By such approximations it is possible to fit the lines of constant cosmic-ray flux at the earth's surface (or equivalently at the top of the atmosphere), the measured cutoff energies, and other data. For example the line of minimum cosmic-ray flux coincides more closely with the dip

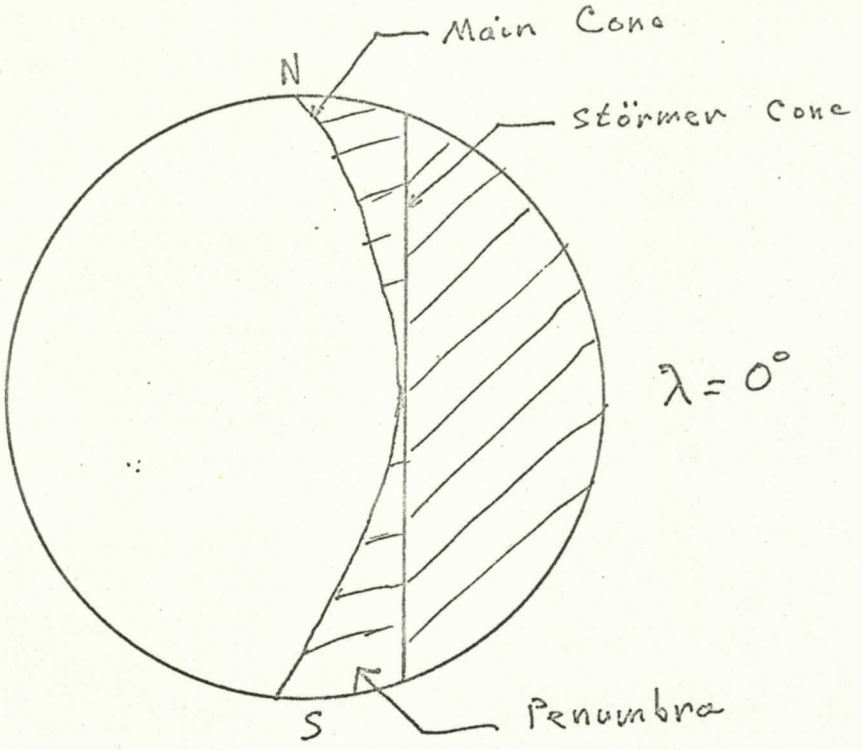

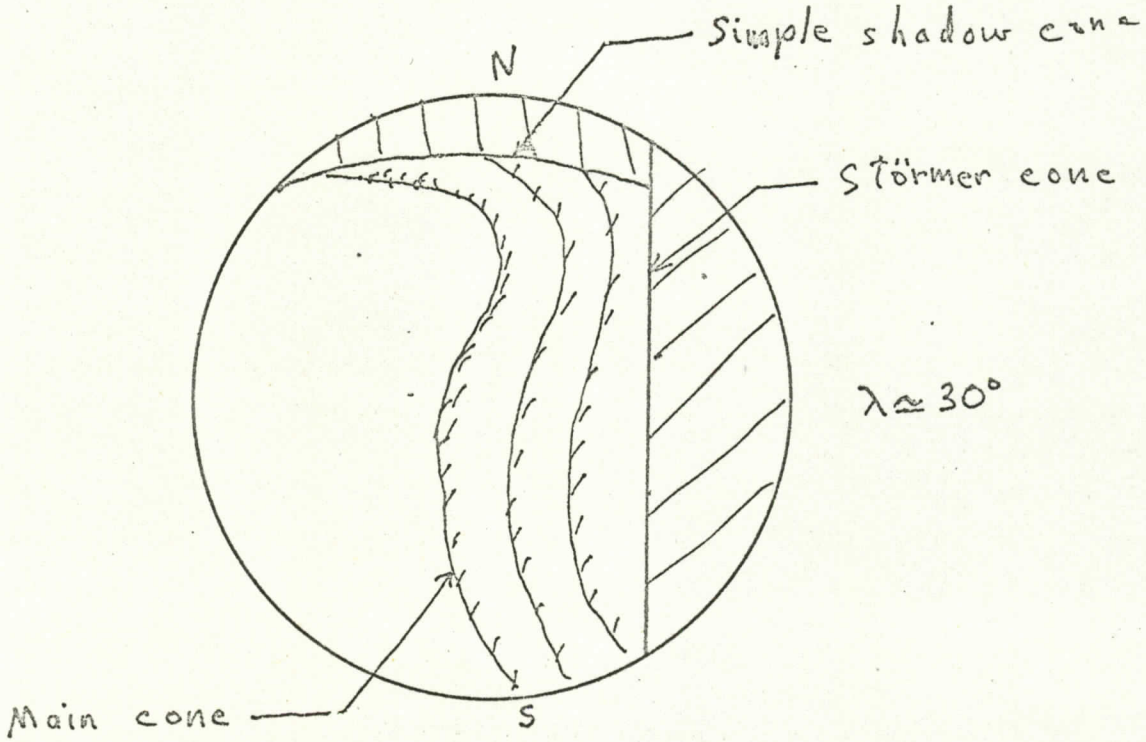

Fig. 12 Allowed Cones

equator than with the geomagnetic equator. On this line the maximum cutoff occurs in the SW Pacific ocean, and the minimum in the South Atlantic. Tables of corrections to simple Störmer cutoffs have been published by Webber and others.

At $\lambda \geq 55^{o}$ the cutoffs are apparently considerably lower than are predicted by even modified Störmer theory, and may in fact be zero over a portion of the polar caps. This is thought to be due to the great distortion of the polar field lines which are stretched some distance into the magnetospheric tail. The exact configuration of the lines, and the resulting cutoff rigidity is not known at present.

References

Stormer, C. The Polar Aurora, Oxford, 1955

Lemaitre and Vallarta, Phys. Rev. 50, 493 (1936).

Webber, W. R., "Time Variation of Low Rigidity Cosmic Rays during the Recent Sunspot Cycle," Prog. in Cosmic-Ray Physics VI, N-Holland Publ. Co. 1962.

19.7 When the cosmic radiation is observed for a long period of time by monitoring stations on the surface of the earth, a number of different variations are seen. The counting rates of such monitors are affected first of all, by the amount of overlying atmosphere, and in the case of muon counters, by the temperature distribution of the atmosphere. The atmosphere varies more or less randomly as the local weather changes, and is also subject to systematic daily changes, seasonal changes, and 11 year (solar activity cycle) changes in response to solar heating. The atmosphere is temporarily affected during solar flare activity due to heating by solar ultra-violet and X radiation. These effects must be removed from cosmic-ray monitor data before the direct effects of solar activity upon cosmic-ray intensity can be studied.

Observations within the magnetosphere frequently make use of the known variation of cosmic-ray cutoff rigidity to determine the rigidity spectrum of the particles in interplanetary space in the range 1 - 15 BV. However, the effects of temporal variations in the shape of the magnetosphere must first be allowed for. The principle effects are first a diurnal variation in cutoff rigidity at latitudes $\lambda \simeq 50\text{-}65^{\circ}$ due to the day-night asymmetry of the magnetosphere. In this region the same cutoff occurs at a higher latitude on the day than on the night side. Secondly, during magnetic storms the latitudes of cutoffs in the range $\sim$ 0.1 - 2 BV move to lower latitude, in effect broadening the polar cap regions. The trapping regions and auoral zones undergo similar changes in latitudinal extent.

19.7.1 In interplanetary space the galactic cosmic radiation has an angular asymmetry and undergoes variations with time. Both of these effects are apparently caused by the interplanetary magnetic field which moves outward with the solar wind. It is thought that in interstellar space, beyond the shock boundary between the solar wind and interstellar medium, cosmic-rays are homogeneous, isotropic, and constant in time over many thousands of years.

At the earths orbit the flux of particles is anisotropic, with the maximum flux coming from a direction in the ecliptic plane $\sim 85^{o}$ east of the sun, on the average. The amplitude of anisotropy is 1/2 to 1% and is independent of rigidity at least over the range 1-200 BV. The variation of the directional flux with direction can be written

$$j(R) = j_{o}(R)[1 + 4 \times 10^{-3} \cos\Lambda \cos(\Psi - 85^{o})]$$

Λ = latitude from ecliptic plane

Ψ = longitude measured from solar direction.

The direction of maximum intensity varies by $\pm \pi/2$ in a matter of days. The anisotropy produces a diurnal variation in the radiation observed at a point fixed on the earth, although the local time of maximum flux depends upon the rigidity observed due to bending of the particle trajectories in the geomagnetic field.

This anisotropy is caused by streaming of the galactic particles inward through the more or less regular spiral of the interplanetary magnetic field.

No sidereal anisotropy has been found, although one might be expected due either to streaming along the magnetic field

in the local spiral arm of the galaxy, to asymmetry in the boundary between the interplanetary and interstellar mediums caused by motion of the sun through the medium, or to a local (galactic) point source of the radiation. Present experiments set on upper limit of 0.1% to the amplitude of the sidereal anisotropy.

19.7.2 The average interplanetary magnetic field has a regular spiral structure, but the actual field has many irregularities that change the direction of drift of fast charged particles so that particles may be regarded as scattering off of the irregularities. This has the effect of making the particles diffuse through the interplanetary medium. Galactic cosmic rays diffuse inward from interstellar space through the medium expanding and flowing outward. This depresses the density of radiation in the medium below the interstellar level by an amount that depends upon the solar wind velocity, average magnetic field strength and turbulence, and the velocity and/or rigidity of the cosmic rays. The best model to describe this process is a subject of considerable current debate. The following discussion is limited to a description of the more important observations.

The number of galactic cosmic rays at the orbit of earth varies with an eleven year periodicity, the minimum intensity occurring approximately when the sun is most active, as measured by sunspot number and average radio noise. The phase of cosmic ray variation lags the solar variation by 6-12 months, this lag being greater during decreasing than increasing solar activity, and greater for lower energy cosmic-rays. Fig. 13 shows the depression

below the 1954 (solar minimum) level of the integral fluxes higher than 1.5 and 14 BeV rigidity.

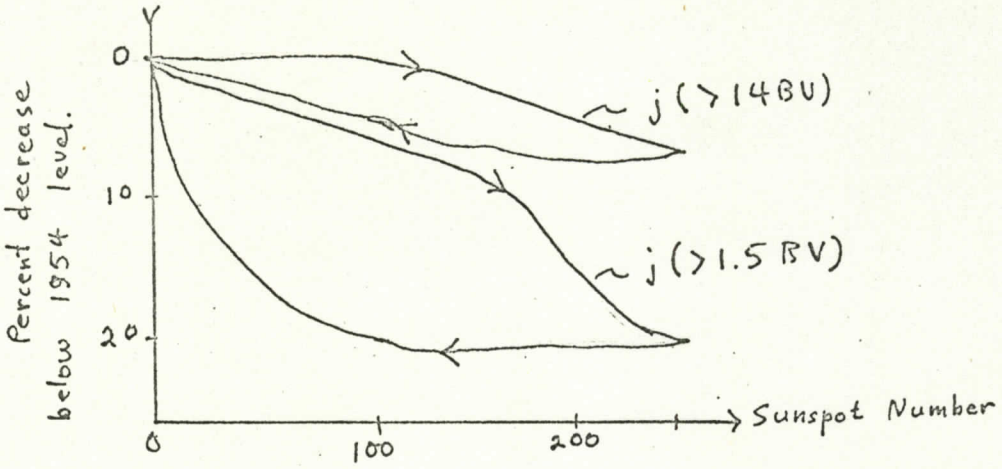

Fig. 13

The depression of the integral flux with R > 0.7 BV was more than a factor of two. Clearly the differential energy or rigidity spectrum assumes different forms during rising and falling solar activity. Fig. 14 shows measured spectra in a few different years. At relativistic energies the rigidity spectra of protons and alpha particles maintain the same shape, the protons being ~ 6 times more numerous, and the spectra are modulated together. At lower energies the spectra are probably modulated differently, although experiments disagree on this. Since the model of diffusion in the interplanetary medium must account for modulation as a function of both rigidity and charge, substantial experimental programs are still underway to measure the modulation.

The depression of cosmic ray intensity inside the solar system below the interstellar level implies that a gradient of intensity with radial distance from the sun must exist at some distance, if not throughout, the interplanetary medium. Experiments

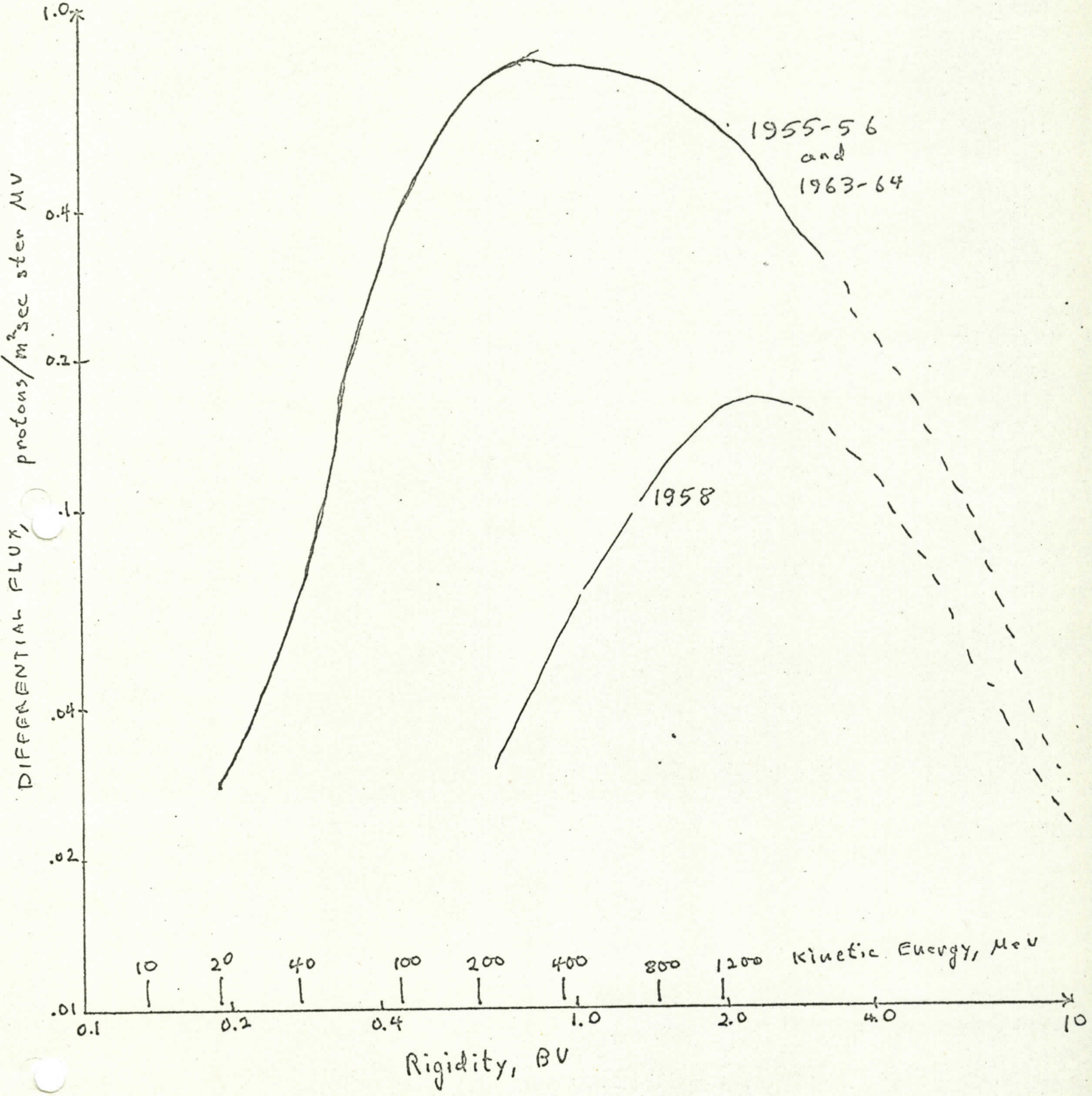
1.0
0.4
0.2
.1
.04
.02
.01
DIFFERENTIAL FLUX, protons/m²sec ster MV
1955-56
and
1963-64
1958
10
20
40
100
200
400
800
1200
Kinetic Energy, MeV
0.1
0.2
0.4
1.0
2.0
4.0
10
Rigidity, BV

Fig. 14.

with interplanetary spacecraft have attempted to measure the gradient. They are not very conclusive, but it seems clear that between 0.75 and 1.5 AU, in the years 1960-1965, the gradient of particles with energies greater than ~ 200 MeV/nucleon (>.65 BV rigidity) was between 0 and 20 percent per A.U. Much larger gradients have been reported in less energetic particles. Since the flux of particles with E > 200 MeV/nucleon varies by more than a factor of two, this small gradient suggests that the modulation extends over a volume 5-10 AU in radius, but the gradient could steepen in some region outside the earth's orbit.

The lag of cosmic ray intensity behind solar activity is often taken to show that the modulated region is large. The lag supposedly corresponds to the time it takes the solar wind to fill the modulated volume. However, no systematic measurements have been made of the interplanetary medium over a solar cycle, and it may be that variations of the solar wind lag 6-12 months behind sunspot activity.

The solar wind does not stop at the time of solar minimum, as evidenced by the continued existence of the magnetopause and bow shock in 1965-66. Hence the cosmic rays may be depressed below the interstellar level even at solar minima like that of 1965. (The minimum sunspot number was greater in 1965 than in 1954). Although the full interstellar flux of relativistic nuclei has probably been seen at earth at solar minimum, we do not at present know what the galactic flux of nuclei or electrons of a few MeV may be. Fig. 15 shows the variation of cosmic radiation within the atmosphere during the past solar cycle.

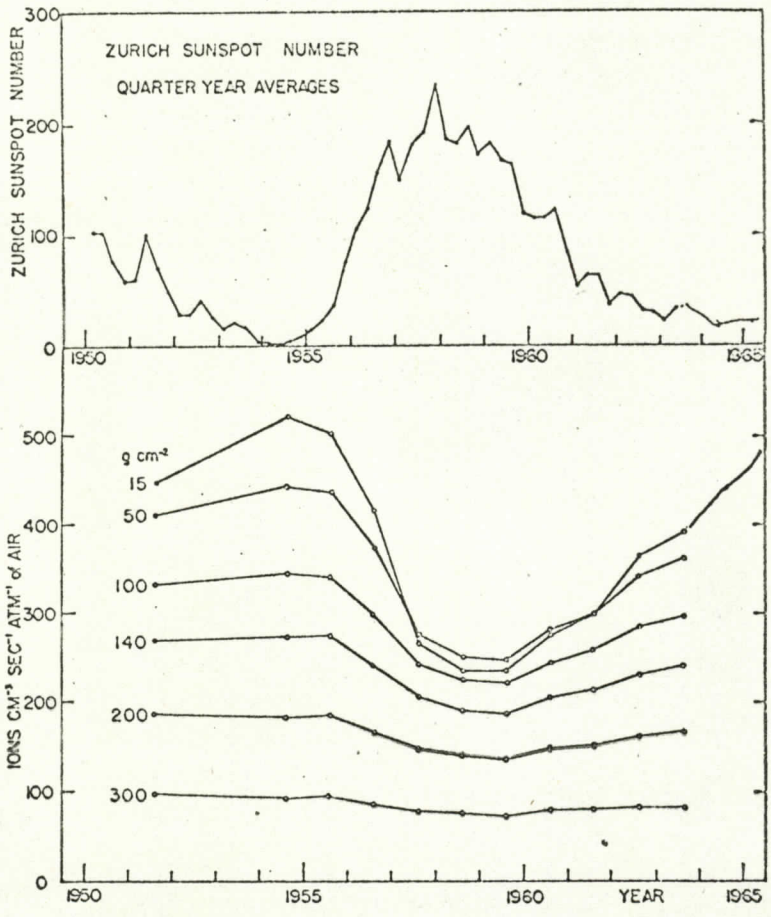
ZURICH SUNSPOT NUMBER
QUARTER YEAR AVERAGES
ZURICH SUNSPOT NUMBER
300
200
100
0
1950
1955
1960
1965
g cm⁻²
15
50
100
140
200
300
IONS CM⁻³ SEC⁻¹ ATM⁻¹ of AIR
500
400
300
200
100
0
1950
1955
1960
YEAR
1965

Fig 15a

IONIZATION vs DEPTH IN ATMOSPHERE AT THULE, GREENLAND

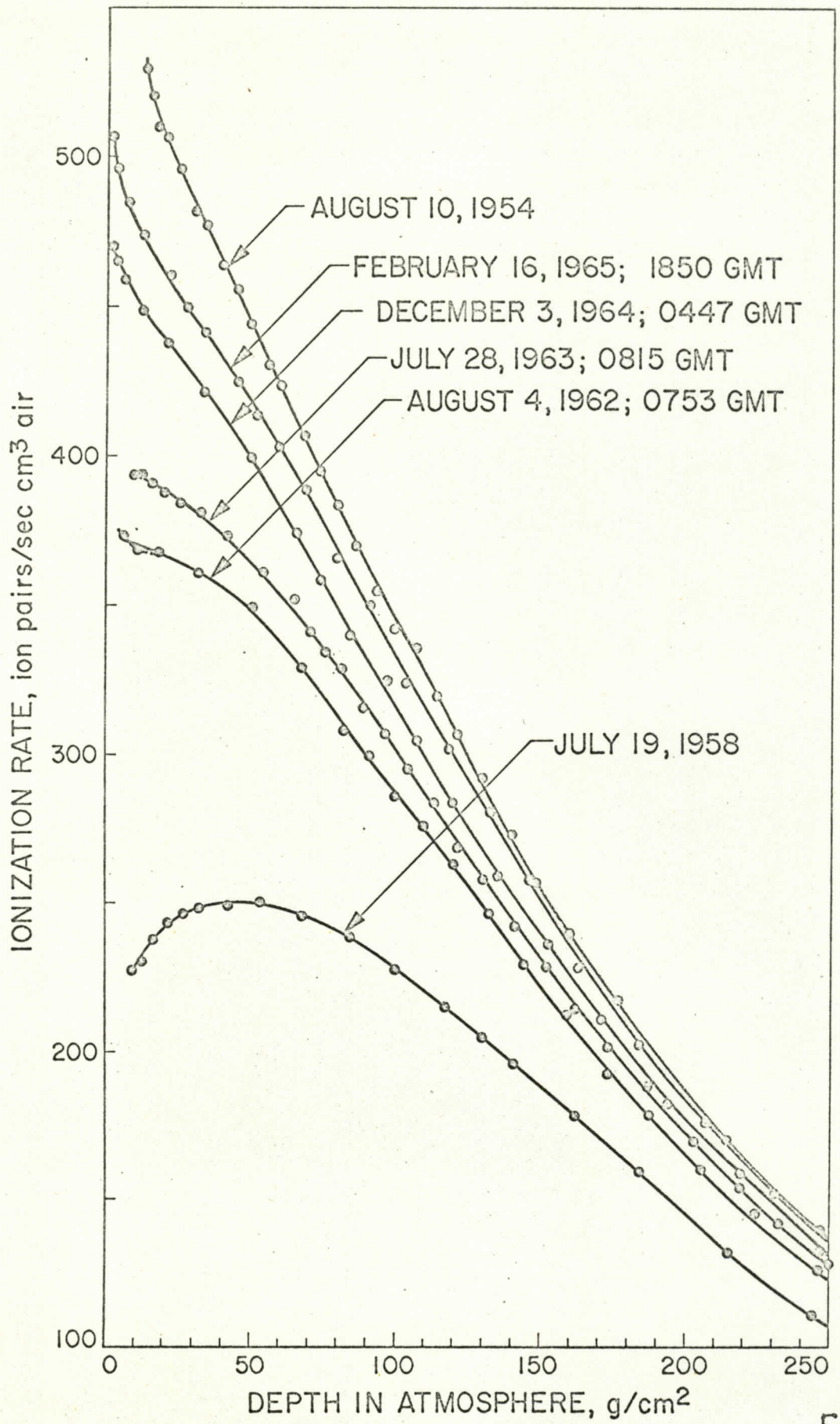

Fig 15 b

In contrast with the gradual eleven year modulation, very rapid variations of the relativistic flux are sometimes observed. The characteristic shape of these Forbush decreases is shown in Fig. 16. The reduction occurs when a stream of solar plasma

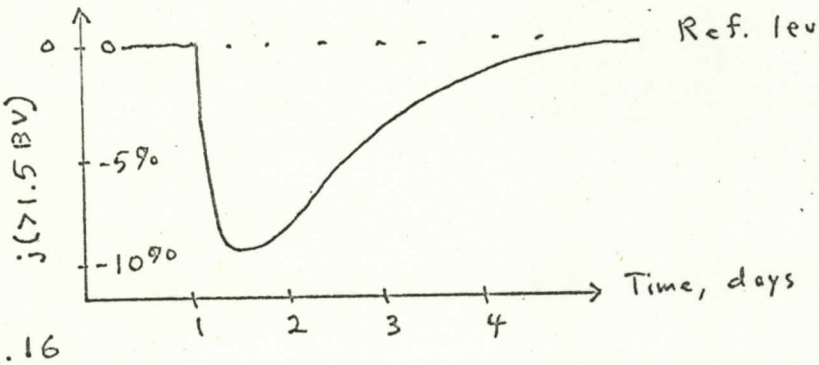

Fig. 16

more rapid than that existing previously, overtakes the point of observation. As such a stream expands, the cosmic ray density in it is temporarily reduced below that in surrounding regions. Recovery occurs as cosmic rays diffuse back in. When such a fast stream envelopes the earth a magnetic disturbance often occurs. Fast streams of plasma are ejected from regions of the sun that frequently persist for several solar rotation. Thus, Forbush decreases often exhibit a 27 day recurrence pattern.

Forbush decreases affect particles with rigidities from a few BV (or possibly less) to over 100 BV, the percentage decrease is approximately proportional to $1/E^{0.9}$. Except during the early, reduction phase the flux remains isotropic.

19.7.3 We have tacitly assumed that the energetic particles normally present outside the magnetosphere come from interstellar space. This is surely so for the majority, but some of the low energy particles may be supplied by the sun. There have been reports that the differential spectra, as shown in Fig. 14, rise again for rigidities lower than 0.2 BV. The existence of a large radial gradient at low energies would argue against this, but the question is not settled.

During certain large disturbances in the solar atmosphere the sun generates a significant number of energetic charged particles. By a mechanism not yet understood energy (probably stored as magnetic field energy) is released in a small region of the solar surface and converts to UV and visible light (a flare) and to kinetic energy of electrons and nuclei. This takes place during a few minutes or hours. The electrons lose much of their energy to synchrotron emission at radio frequencies, as they spiral in the surface magnetic field, and to bremstrahlung x-rays. Some escape into interplanetary space from the strong field of the flare region, and many of the nuclei escape. The flare often occurs in a disturbed region that has existed for some time. Sometimes the region also emits a high speed stream of plasmas after the flare occurs.

At the earth (or other observation point) electromagnetic radiation from the flare is observed promptly, and charged particles after a delay of 10-60 minutes. Fast particles arrive first, and the slower ones do not reach a peak until many hours later. The time history of arrival depends upon the configuration of magnetic field that connects the flare region and the earth, or point of observation. Arrival is most prompt if the field is smooth and the earth is on a tube of force that connects with the active regions. This requires that the flare occur on the western portion of the visible disc as seen from Earth. When there is a direct connection the prompt radiation may reach the earth along the direction of the local interplanetary field so that a maximum of intensity is observed in a direction $\sim 50^{o}$ west of the sun. As the particles diffuse beyond the earth and are reflected back the flux becomes isotropic, and remains so

during the decay of the flux. In other cases only isotropic fluxes are observed, and these arrive more slowly. Fig. 17 shows possible field configurations.

At the earth the energy (or rigidity) spectrum varies during an event and from event to event. In general energetic particles arrive first with slower ones reaching a peak flux later. After the peak intensity has been reached, the integral spectrum may often be represented by $j(>E) = K/E^n$ with $n = 4$ to 6, but below 10 MeV the spectra probably flatten. The form $J(>R) = Ke^{-R/R_o}$ sometimes appears to fit the data better. Fig.18 shows the development of the energy spectrum during an event, and Fig. 19 exhibits two measured spectra in comparison with galactic cosmic rays.

The fluxes decay with a dependence on time that varies between $1/t^{3/2}$ and e^{-t/t_o}, the former describing diffusion into an infinite diffusing medium, and the latter, leakage from a trapping region. Again, the behavior of the radiation depends upon the condition of the interplanetary medium. When the flare region begins emitting a stream of fast plasma, the stream may reach the earth about a day after the flare. When this happens the rate of flux decay may change, and fresh low energy particles (several MeV) may be carried in the stream. These are called solar storm particles, and if the plasma stream persists, may reappear after 27 days. The plasma stream may cause Forbush decreases of galactic cosmic rays.

The ratio of protons to α particles in solar cosmic ray fluxes ranges from 30:1 to 1:1, but the distribution of $Z \geq 2$

nuclei is about that shown in Table I, and is about the same as the solar abundance. The electron to proton ratio varies but is usually small.

Solar cosmic-rays can be detected at Earth by instruments above the atmosphere at high latitudes, and occasionally, when very high energy particles occur, by monitors on the surface. A powerful technique uses the riometer, a receiver that records cosmic radio noise in the 1-50 mc range. When energetic particles cause additional ionization in the low ionsophere, absorption of the noise increases in proportion to the extra electron density, n. When the sun illuminates the atmosphere, so that negative ions, which lead to recombination, are promptly photoionized, the electron density is given approximately by

$$\frac{dn}{dt} = kJ - \alpha n^2 \qquad J = \text{solar particle flux}$$

$$= 0 \text{ at equilibrium} \qquad k, \alpha \text{ are constants}$$

$$\therefore \quad n = \sqrt{\frac{k}{\alpha} J} \propto \text{to absorption}$$

Particles with energies down to ~ 10 MeV are effective, and the method can detect fluxes as small as

$$j(>10 \text{ MeV}) \sim 1/\text{cm}^2 \text{sec ster.}$$

The radio absorption occurs uniformly over the polar regions at latitudes higher than that where the cutoff is ~ 10 MeV. Hence the solar cosmic ray events are called polar cap absorption (PCA) events. Variations of the region covered by PCA reflect both changes in the solar cosmic ray spectrum and in the magnetosphere. Figure 20 shows the sequence of events that may occur

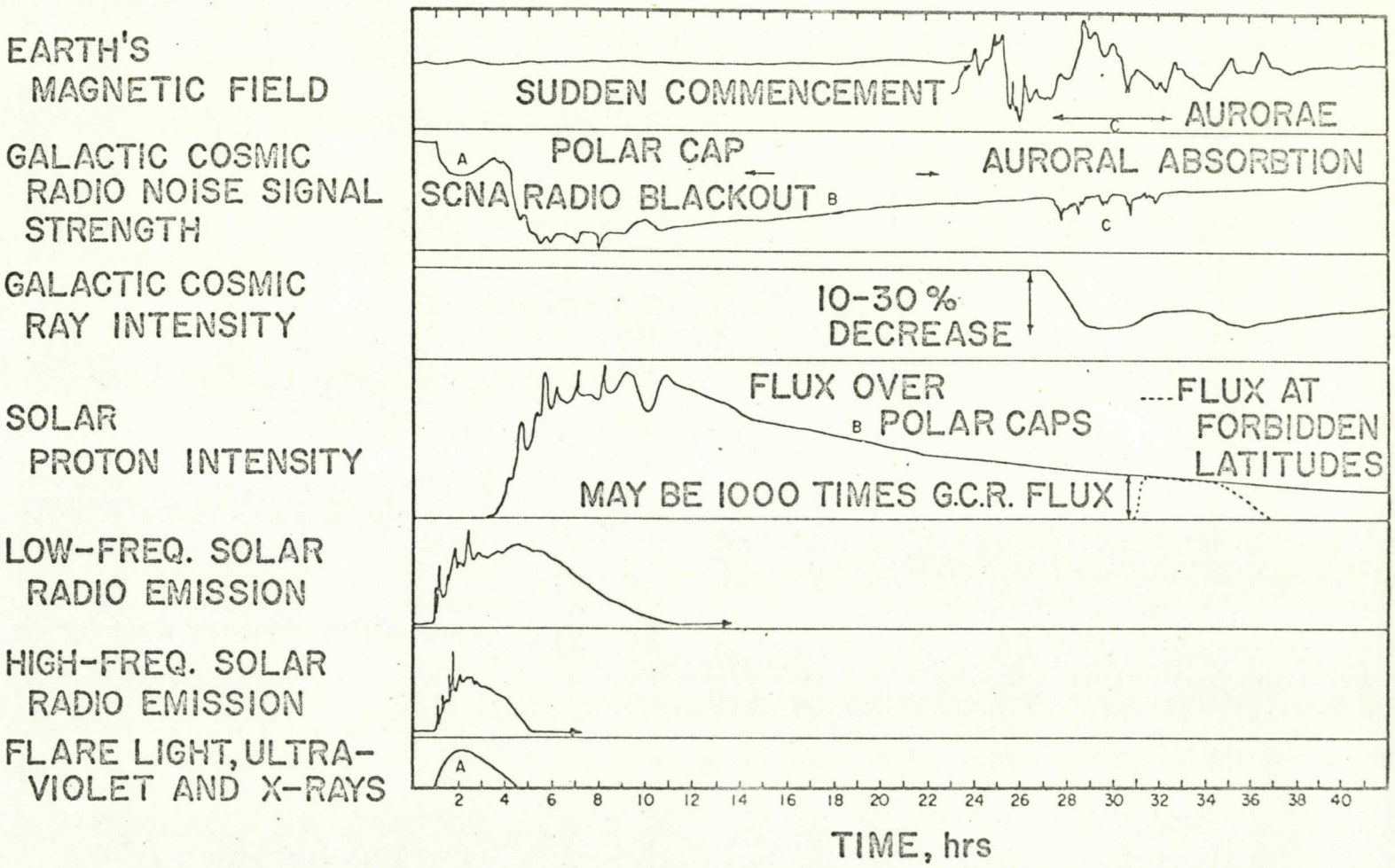
EARTH'S MAGNETIC FIELD
SUDDEN COMMENCEMENT
AURORAE
C
GALACTIC COSMIC RADIO NOISE SIGNAL STRENGTH
A
POLAR CAP
AURORAL ABSORBTION
SCNA
RADIO BLACKOUT
B
C
GALACTIC COSMIC RAY INTENSITY
10-30 % DECREASE
SOLAR PROTON INTENSITY
FLUX OVER
B POLAR CAPS
....FLUX AT FORBIDDEN LATITUDES
MAY BE 1000 TIMES G.C.R. FLUX
LOW-FREQ. SOLAR RADIO EMISSION
HIGH-FREQ. SOLAR RADIO EMISSION
FLARE LIGHT, ULTRA-VIOLET AND X-RAYS
A
2 4 6 8 10 12 14 16 18 20 22 24 26 28 30 32 34 36 38 40
TIME, hrs

Fig 20

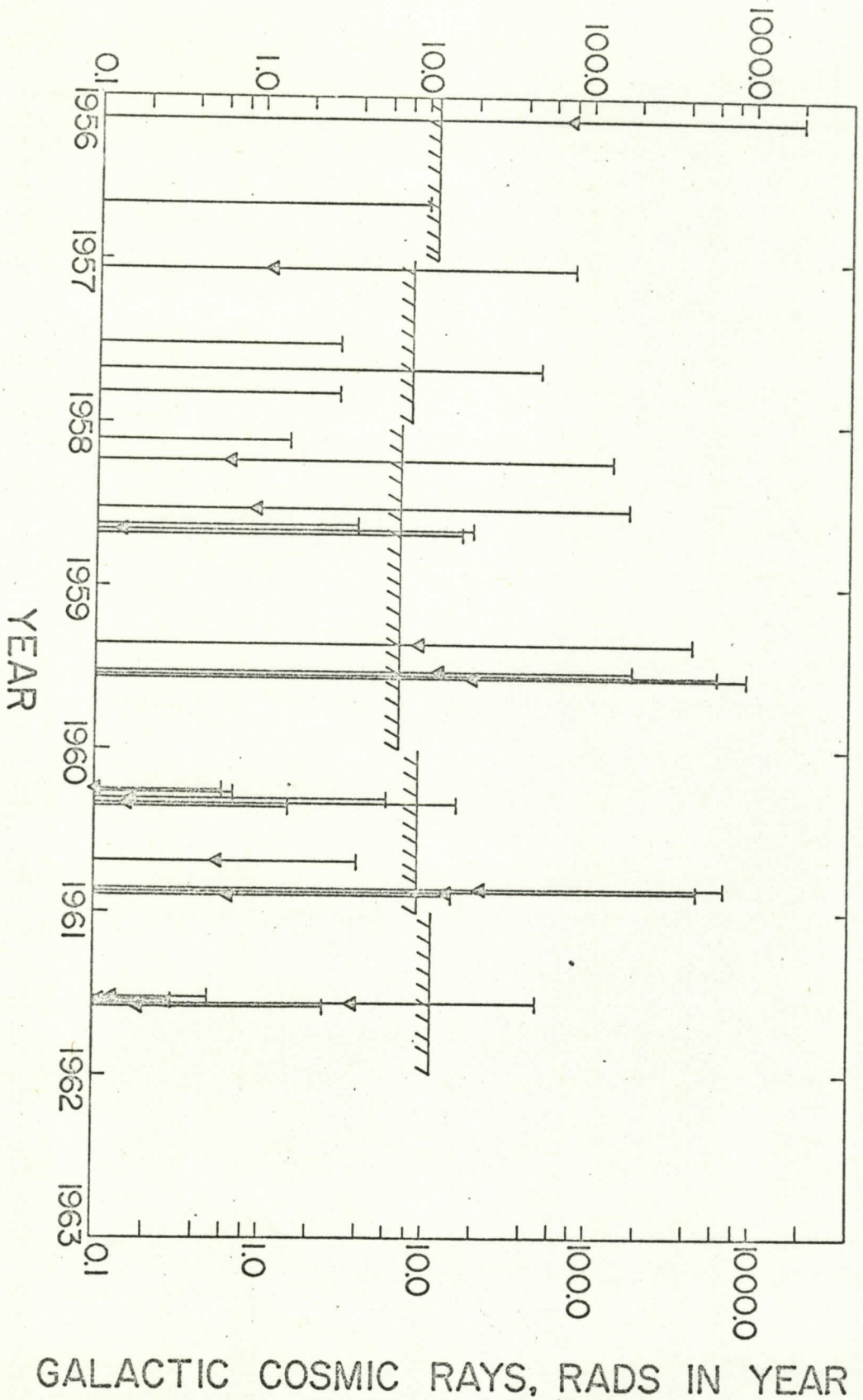
RADS IN EVENT
0.1
1.0
10.0
100.0
1000.0
YEAR
1956
1957
1958
1959
1960
1961
1962
1963
GALACTIC COSMIC RAYS, RADS IN YEAR

Fig. 21

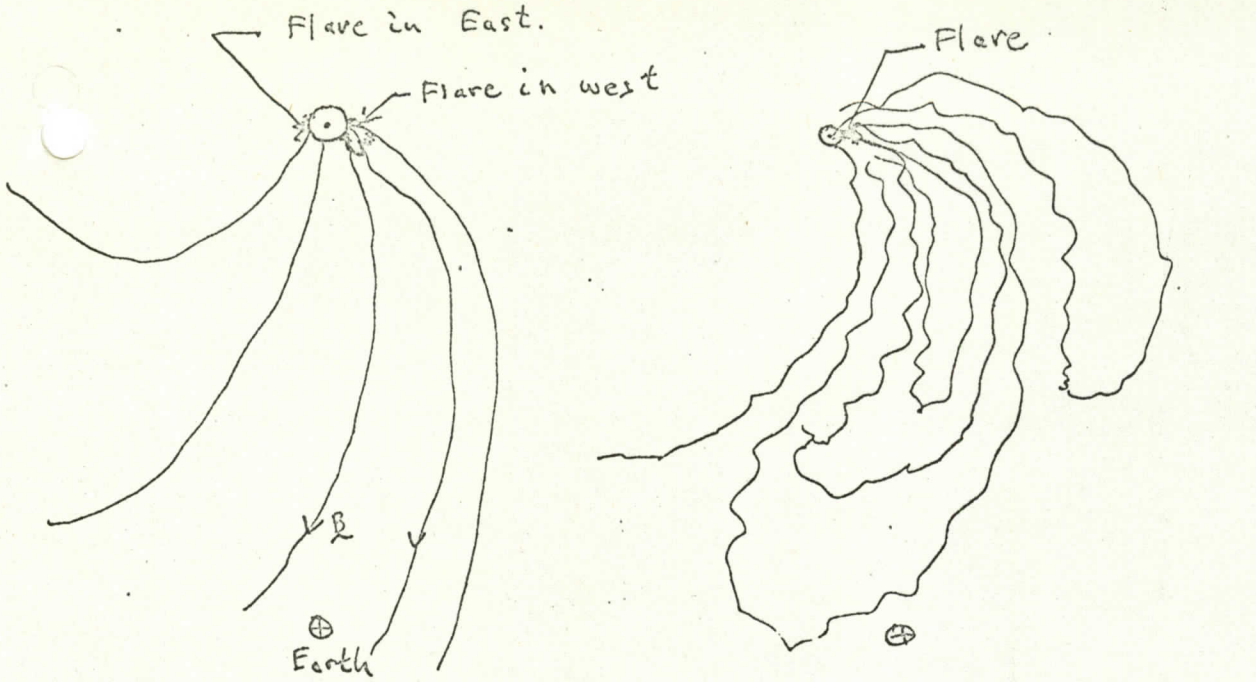

Fig 17

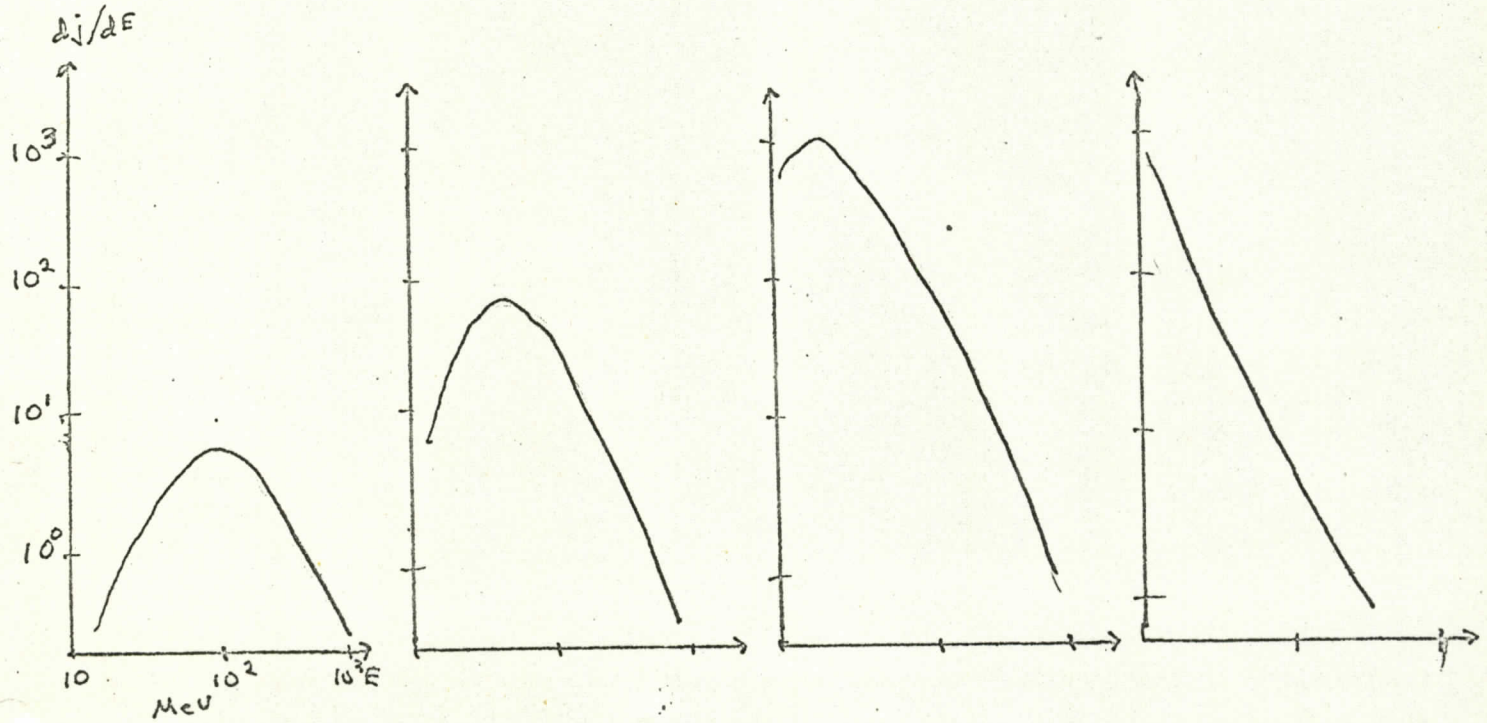

Fig 18. Developement of solar proton spectra.

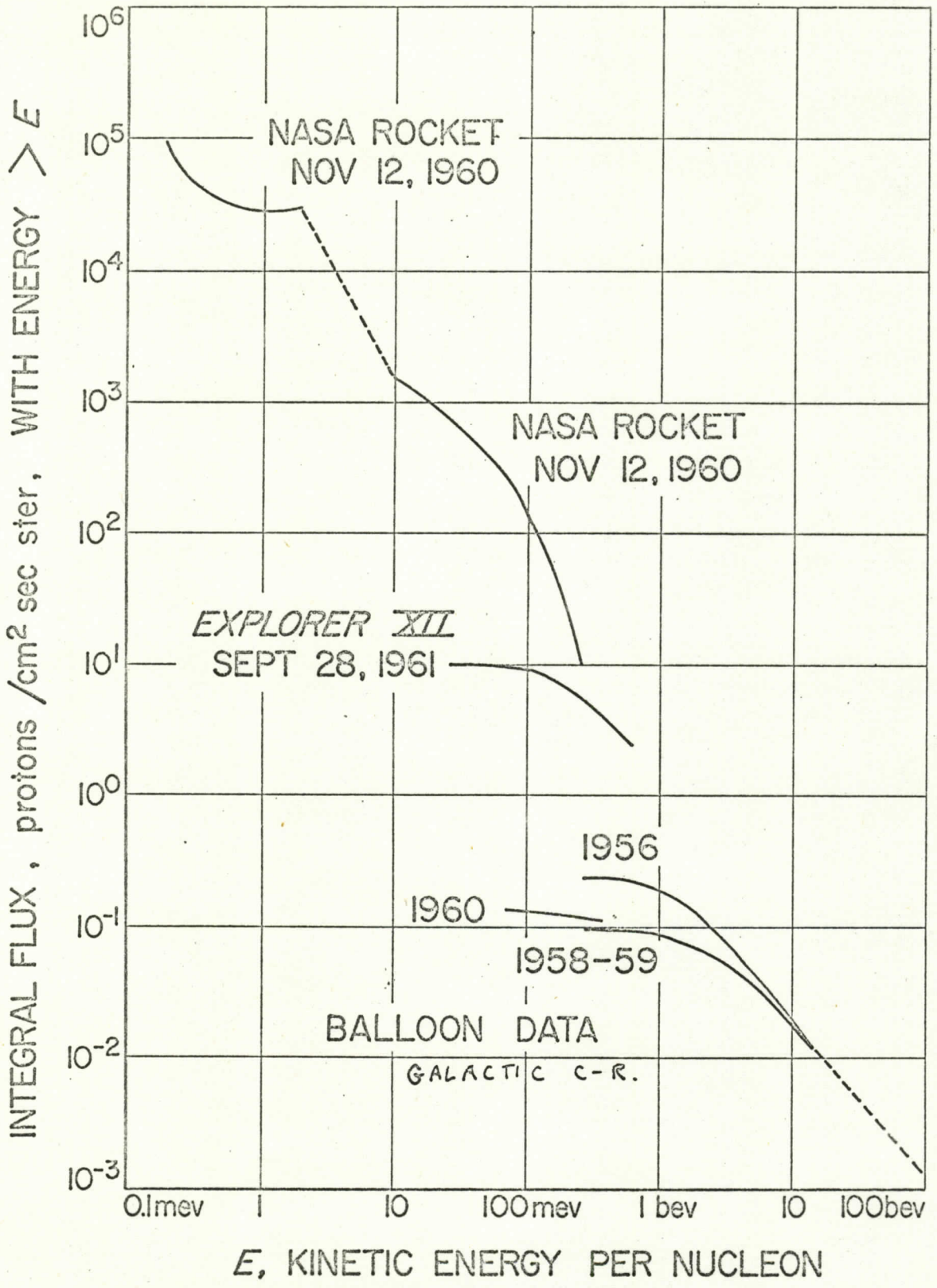
INTEGRAL FLUX , protons /cm² sec ster, WITH ENERGY > E
10⁶
10⁵
10⁴
10³
10²
10¹
10⁰
10⁻¹
10⁻²
10⁻³
NASA ROCKET
NOV 12, 1960
NASA ROCKET
NOV 12, 1960
EXPLORER XII
SEPT 28, 1961
1956
1960
1958-59
BALLOON DATA
GALACTIC C-R.
0.1mev
1
10
100mev
1 bev
10
100bev
E, KINETIC ENERGY PER NUCLEON

Fig 19

at Earth during a solar proton event.

The radiation dose due to cosmic rays in interplanetary space is sometimes of interest. Behind more than a few mils of material solar cosmic rays contribute only during a few very large events. In Fig. 21 we show the dose due to galactic cosmic rays, and to solar cosmic rays with $E > 30$ MeV (tops of bars) and $E > 100$ MeV (triangles on bars).

Ref.

W. R. Webber, ibid.

19.8 The origin of cosmic radiation is not known, it should be made clear at the outset, and current theories can only list the requirements on a source, or sources, and offer reasonable possibilities. It is clear that most cosmic rays are accelerated by electromagnetic processes and not directly by nuclear or thermal (statistical collision) processes. Although some detailed mechanisms for e-m acceleration have been described, notably by Fermi, we do not expect to find the precise mechanisms of acceleration. Indeed, we cannot do this for acceleration within the earth's magnetosphere.

19.8.1 The principal features of the radiation that must be accounted for are these:

1) The approximate constancy of the radiation (neglecting solar modulation of course) over at least many thousands of years, as deduced from C^{14} and meteorite data. The source must be either continual or if impulsive have been long ago or else be repetitive and distant.

2) The isotropy of the flux, even up to the highest observed energies of 10^{19} - 10^{20} eV. This seems to require either that

a) Both galactic and intergalactic space be filled uniformly with cosmic rays;

b) Or, that the interstellar magnetic field be stronger than the most likely value of $\sim 5 \times 10^{-6}$ gauss;

c) Or, that cosmic-rays fill the galactic halo (the spherical non-thermal radio noise halo) and the disc of stars. Otherwise the flux of the higher energy particles would be greater in the galactic plane than perpendicular

to it for those particles whose orbital radius of curvature in the field is greater than the thickness of the disc. The dimensions of the galaxy are shown in Figure 22.

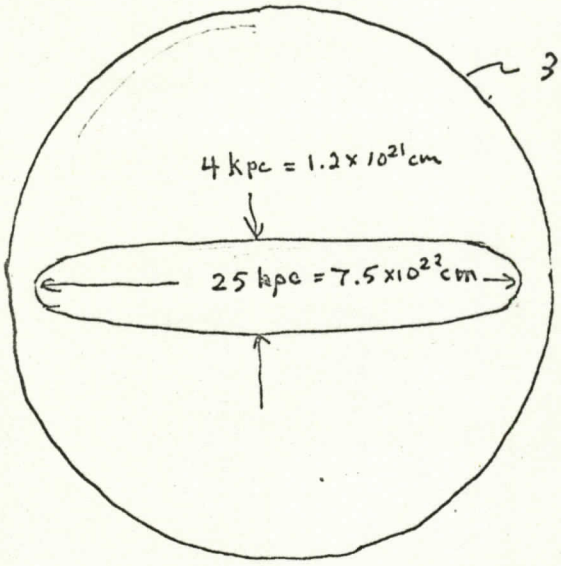

Average $|\underset{\sim}{B}|$ in disc 5×10^{-6} gauss
in halo 1×10^{-6} gauss

The maximum rigidities a particle can have for various turning radii, δ , are listed below

B \ δ	2 kpc	15 kpc
5×10^{-6}	9×10^{17} eV	7×10^{18}
10^{-6}	1.8×10^{17}	1.4×10^{18}

These are equal numerically to the energies of protons so that there is a problem of containing the highest energies even in the halo. If the high energy primaries are fully ionized

heavy nuclei the problem is somewhat alleviated.

3) The charge spectrum of cosmic rays, which seems to retain the same distribution of nuclei at all energies studied. (Charges have been measured only up to $\sim 10^{11}$eV). The chief problem here is that nuclei with Z = 2 to ~ 10 are more abundant compared with heavier nuclei than is the case with the "universal" abundances. This is particularly so with Li, Be, B, which are generally very rare. This requires either that the sources of cosmic rays are enriched in light nuclei, or, as seems more likely, that heavy nuclei such as iron, and perhaps protons and alphas, are accelerated and the heavy nuclei are fragmented into lighter nuclei as the cosmic rays pass through interstellar matter. Passage through 5-15 g/cm^2 of matter is required. With an estimated interstellar gas density of 10^{-26} and 10^{-24} g/cm^3 in the halo and disc, respectively, the cosmic rays must have traveled 5×10^6 to 10^9 ly, and have lifetimes of an equal number of years. This may be termed the mean nuclear lifetime. Heavy nuclei have a shorter average lifetime than the light ones.

a) If it is supposed that cosmic rays are accelerated inside the galaxy and ultimately leak out into intergalactic space, then the lifetime against leakage must approximate the nuclear lifetime in order for the fragmentation hypothesis to be tenable. This apparently requires storage in a spherical volume, and not just in the galactic disc.

The leakage lifetime from the spherical galaxy is estimated to be $\sim 3 \times 10^8$ years, which is adequate.

b) The fragmentation hypothesis predicts two other phenomena that are in principle observable. Decay of π^o produced in collisions must generate a flux of hard gamma rays which is, however, at least two orders of magnitude less than the experimentally determined upper limit. In addition secondary electrons and positrons, in approximately equal numbers, must result from the decay of $\pi^{\pm}$ produced in nuclear collisions. The differential energy spectrum of secondary electrons resembles that of primary nuclei and is proportional to $E^{-\gamma}$ with $\gamma \simeq 2.7$. The observed galactic electron flux is an order of magnitude larger than the calculated secondary flux, has approximately equal numbers of e^+ and e^-, and a $\gamma = 1.7$. It is concluded that most of these electrons have another origin and are probably accelerated electromagnetically.

4) The energy spectrum and total energy content of the rays. Their energy density w_{cr} is ~ 1 ev/cm^3, about equal to the energy density of the interstellar magnetic field, of the motion of gas clouds, and of starlight. The total rate of energy loss by cosmic rays, and of energy input to them, Q_{cr}, is therefore

$$Q_{cr} \simeq \frac{w_{cr}\ \mathrm{Vol}_{galaxy}}{\tau_{cr}} = \frac{1 \times 4\pi/3\ (4\times10^{22})^3}{10^{14} \text{ to } 10^{16}}$$

$$= \frac{2\times10^{68}}{10^{14} \text{ to } 10^{16}} = 10^{54} \text{ to } 10^{52} \text{ ev/sec.}$$

$$= 10^{42} \text{ to } 10^{40} \text{ erg/sec}$$

19.8.2 Before discussing possible origins of the cosmic radiation, it is important to consider the galactic electron and gamma flux. Measurements of very relativistic electrons are few. Three available measurements are

$$j\ (> 0.5\ \text{BeV}) = 3.2 \pm 1.0/\ m^2 \text{sec ster}$$

$$j\ (> 5.3\ \text{BeV}) = 6.8 \pm .6/\ m^2 \text{sec ster}$$

$$\frac{dj}{dE} = \frac{11}{E^{1.6}}\ /m^2 \text{sec ster BeV}.$$

which are in rough agreement, and amount to about 1% of the proton flux. Negatrons appear to predominate. As noted, this flux is larger than the calculated secondary flux. According to some calculations this flux is sufficient to generate the non-thermal galactic radio noise, (see section 20) but other analyses show that it is a factor of ten too small. If this is the case, it could be that the interplanetary medium inhibits some electrons from reaching the earth's orbit, but if this is so, nuclei with rigidities of a few BV must be similarly inhibited. A further burden is thrown on theories of cosmic ray origin if the interstellar flux is a factor of ten higher than the terrestrial value at solar minimum, which is normally adopted.

The non-thermal radio noise is further significant to an understanding of nuclear cosmic rays because the existence of the galactic halo is inferred from its angular distribution and because the existence of point sources of radio noise (such as the Crab Nebula) implies sources of relativistic electrons. It is supposed that such objects may be sources of nuclear cosmic rays also.

Gamma rays result from three processes involving cosmic ray particles. Nuclear collisions produce π^o which decay; cosmic ray electrons collide with interstellar gas to produce bremsstrahlung, and accelerate visible light photons to gamma ray energies in inverse Compton collisions. The calculated number of gamma rays is small, as the table below shows.

Production Process	Flux, photons/cm^2 sec ster E_γ>50 MeV	E_γ>1 BeV
$\pi^o \rightarrow 2\gamma$	6.6×10^{-6}	4.5×10^{-7}
Bremsstr.	9.6×10^{-6}	4.8×10^{-7}
Inverse Compton	10^{-4}	2×10^{-5}

An experimental upper limit to the flux with E_γ>50 MeV is 3×10^{-4}/cm^2 sec ster.

The total energy of non-thermal radio noise emission from the galaxy is $\sim 3 \times 10^{38}$ erg/sec, no more than 1% of the cosmic ray energy loss. The energy lost by electrons to inverse Compton collisions is estimated to be 3×10^{39} erg/sec. Thus, if a mechanism that accelerates cosmic-ray nuclei can be found, it is no additional energy burden for it to accelerate electrons.

19.8.3 Various locations and mechanisms for acceleration have been proposed, and doubtless all of them contribute somewhat, although it is presently thought that supernovae predominate.

1) The Fermi mechanism is statistical and produces a $E^{-\gamma}$ energy spectrum. According to it, moving interstellar clouds of gas contain regions of higher than average magnetic field which reflect cosmic rays. The latter gain or lose energy

depending upon whether the collisions are headon or overtaking. The former are more likely, and so there is an average acceleration. If v = cosmic ray velocity, V = gas cloud velocity, λ = mfp between collisions with clouds, and τ = mean life of a cosmic ray, then the average rate of energy gain in the non-relativistic approximation is

$$\frac{dE}{dt} \simeq 4 \frac{EV^2}{\lambda c} \frac{v}{c}$$

which gives

$$E = E_o e^{\alpha t} \qquad , \alpha = \frac{2V^2}{\lambda} \frac{v}{c^2}$$

If N = number of cosmic rays, then their lifetime is given by

$$\frac{dN}{N} = -\frac{dt}{\tau} \quad \text{or} \quad N(>t) = N_o e^{-t/\tau}$$

Putting these together gives $N(>E) = N_o \left(\frac{E_o}{E}\right)^{1/\alpha\tau}$.

This mechanism is not sufficient because the slope of the energy spectrum is greater for smaller τ, and should therefore be greater for heavy nuclei than for light if τ is a nuclear lifetime rather than a diffusive loss lifetime. It also fails because the acceleration is too slow in the known interstellar conditions.

2) The sun accelerates energetic particles occasionally, the average energy generation being 10^{23} erg/sec. There are 10^{11} sun-like stars in the galaxy, so their total energy generation must be $\sim 10^{34}$ erg/sec $<< 10^{40}$. Also, the energy spectrum of solar cosmic rays is wrong, so sun-like stars do not produce many galactic cosmic rays. Various special

classes of stars fall similarly short, with the exception of novae and supernovae.

3) Supernovae occur about once in 100 years = 3×10^9 sec in the galaxy and, it is estimated, produce $\sim 6 \times 10^{50}$ ergs each, of which $10^{47} - 10^{48}$ ergs goes into relativistic electrons and ultimately synchrotron emission of radiation. If we assume that 100 times as much energy goes into relativistic nuclei, then the average cosmic-ray energy production is

$$Q_{cr} = \frac{10^{49} - 10^{59} \text{ erg}}{3 \times 10^9 \text{ sec}} = 3 \times 10^{39} \text{ to } 3 \times 10^{40} \text{ erg/sec}$$

which is about enough energy! It should be noted also, that the radii of supernovae shells are 1-2 pc and the average $B \simeq 10^{-3}$ gauss, so protons up to 10^{17} to 10^{18} eV could be contained.

For these reasons, supernovae are thought to be the principal source of cosmic ray nuclei and electrons.

4) Novae develop 10^{-4} to 10^{-5} the energy of supernovae but are 10^4 times as frequent. However, there is no evidence of relativistic electrons in novae.

In conclusion it must be stressed that the above outline may be subject to many errors. More complete theoretical analyses of motion in the interstellar medium might lead to different conclusions. New experimental data on the energy spectra of heavy cosmic ray nuclei and of fast electrons will be of great interest when it becomes available.

Ref: Ginzburg, V. L. and S. I. Syrovotskii, The Origin of Cosmic Rays, Macmillan, New York, 1964.